CHAPTER 12: BEAM INSTABILITIES

M. FURMAN, J. BYRD AND S. CHATTOPADHYAY*

Center for Beam Physics
Accelerator and Fusion Research Division
Lawrence Berkeley Laboratory
University of California,
Berkeley, CA 94720, U.S.A.

12.1 Introduction

So far we have considered the motion of the particles in the accelerator in given external electric and magnetic fields. As the particles traverse the ring, however, they interact with their surroundings via the electromagnetic field created by their own charge and current. This field extends for a certain distance behind the particles that created it, and is called the *wake field*. As an example of this interaction, the resistivity of the vacuum chamber causes ohmic losses as the wake field drags along the image currents in the wall of the chamber. In addition, the wake field can act back on the same bunch that created it and/or on the other bunches that come behind. Or, as a bunch traverses an RF cavity, it can excite one or more of its higher-order modes (HOMs); although the electromagnetic fields of these modes are mostly trapped inside the cavity, they typically resonate for a long time, and can therefore influence all the bunches in the beam as they, in turn, traverse the cavity. Thus in general, if certain conditions are met, the wake field can act back on the beam in such a way that an initial disturbance gets amplified and hence an instability is generated. In some cases, the disturbance grows indefinitely, causing beam loss; in others, the disturbance saturates, growing only until a new equilibrium situation is reached.

The key signature for these phenomena is an *intensity dependence*: when the current is low the wake fields are weak, and the beam characteristics are dominated by single-particle dynamics. As the beam current is increased, the wake fields become stronger and can influence the beam dynamics, and hence the machine performance, significantly. Some of these phenomena depend smoothly on current, and some others have a well-defined onset as the current exceeds a threshold value beyond which the wake field forces overcome the damping mechanisms. All of these phenomena arise because the beam, being a collection of charges, acts back on itself via the environment in which it travels; for this reason, these are called *collective phenomena*.

In this chapter we present an outline of the typical instabilities observed or expected in light-source synchrotrons and the techniques used to avoid or mitigate them. Since the physics of

* Work supported by the Director, Office of Energy Research, Office of High Energy and Nuclear Physics, High Energy Physics Division, of the U.S. Department of Energy under Contract no. DE-AC03-76SF00098. Fax: (510) 486-7981. E-mail addresses: miguel@lbl.gov, jbyrd@lbl.gov and chapon@lbl.gov. Published in Synchrotron Radiation Sources: A Primer, H. Winick, editor (World Scientific, 1994).

instabilities is generic to all rings that store relativistic electrons or positrons, it is important to note that the situation in light sources is very similar to what is found in other circular machines such as damping rings and e^+-e^- colliders.

At the core of any discussion on instabilities is the *impedance of the machine*, which is closely related to the wake field. Once the impedance is known, it is possible to calculate the thresholds and growth rates of the instabilities. The definition of impedance and a discussion of its properties and measurement techniques is presented later.

We also describe briefly ion trapping, intrabeam scattering and Touschek scattering. Although these phenomena do not depend critically on the interaction of the beam with its surroundings, they are nevertheless intensity dependent, and in this sense they can be considered collective effects.

12.1.1 Stability[1]

The actual closed orbit in a real machine deviates from the ideal closed orbit due to inevitable errors in survey and alignment. Typically, the maximum value of this deviation could range from a few mm to a cm, arising from a realistically achievable survey and alignment error of 0.1 mm. This is a time-independent, stationary configuration and can be improved by a closed-orbit measurement and correction scheme, employed in all modern storage rings. An irreducible residue of 0.1–0.5 mm in the maximum closed-orbit deviation is achievable after a convergent series of iterations.

Machine operation would be simple if the orbit, the lattice functions and the RF parameters were independent of time and particle oscillations were linear to large amplitudes. The challenge of control of the photon source stems from the reality of time-dependent perturbations and the essential nonlinearity of the beam dynamics at large amplitudes. There is always long-term ground motion and various vibrations and noise sources at shorter time scales, and particles are subjected to large oscillation amplitudes at injection as well as during the rest of the lifetime of the beam by various scattering processes. In addition, there are other time-dependent processes, such as coherent beam instabilities, oscillations of trapped ions interacting with the beam, etc. The frequencies and time scales of these various processes, their sources, manifestations in the beam and ring properties, monitoring systems and possible cures can be grasped by a look at Fig. 12.1

12.1.2 Overview of Instabilities and Their Effects

Instabilities are usually classified into single-bunch and multi-bunch. Single-bunch instabilities are strongly influenced by short-range wake fields arising from small structures in the vacuum chamber such as bellows, discontinuities, vacuum ports, beam position monitors, etc. Multi-bunch instabilities are strongly influenced by long-range wakefields, or by localized wake fields that last for a long time. As mentioned above, the most important mechanism that gives rise to such wakefields is the excitation of HOMs in resonant structures, especially the RF cavities. The wake

fields produced by the finite resistivity of the vacuum chamber are also important in this respect.

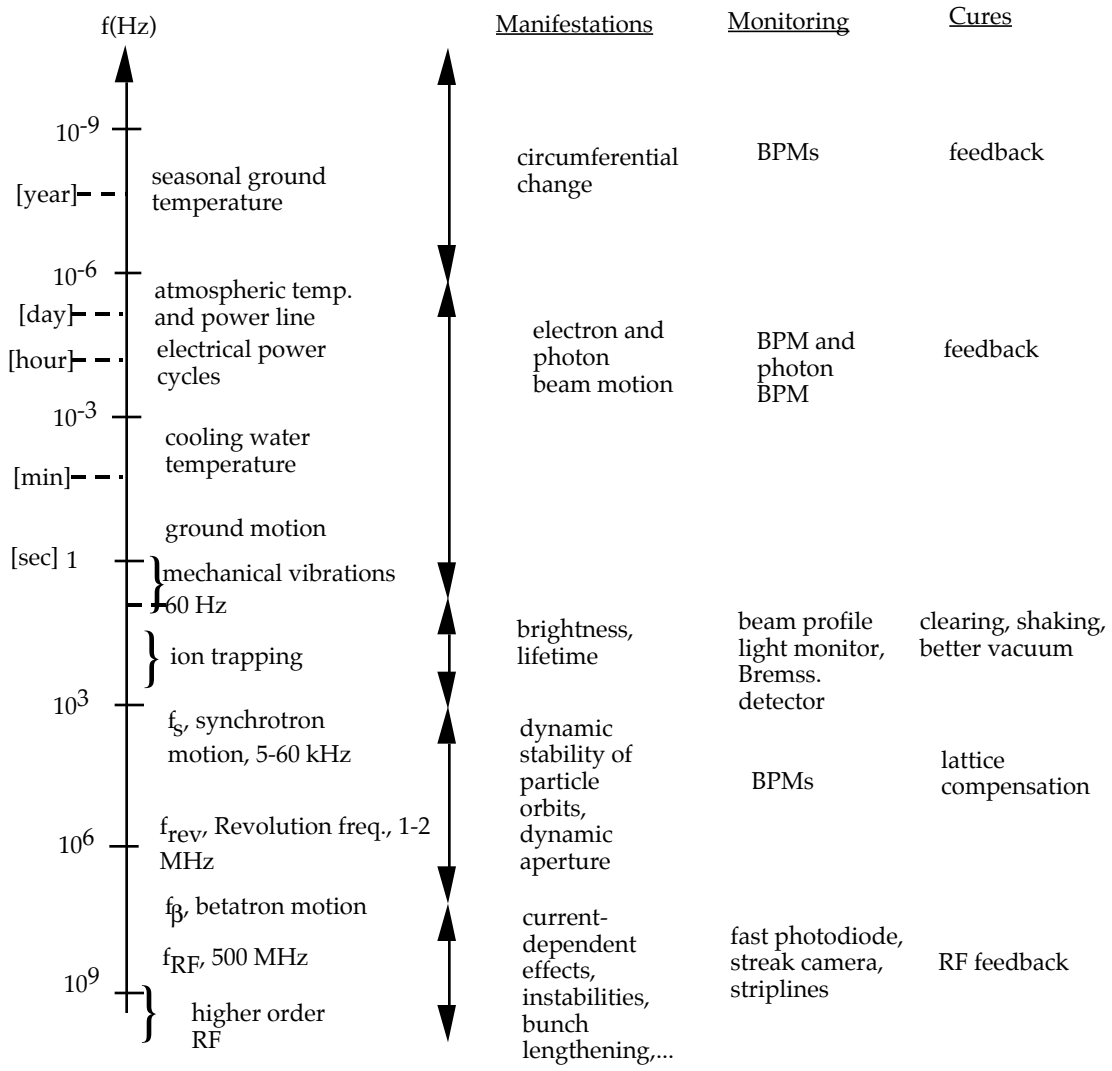

Fig. 12.1. Various frequencies and time scales relevant to storage-ring stability.

Instabilities can have two kinds of unfavorable effects: degradation of the beam lifetime, and degradation of the beam quality. These two effects are not mutually exclusive. Typical design goals of light sources are long beam lifetime, small beam emittance, short bunch length, small energy spread and stable orbits. Instabilities can cause bunch lengthening, increased energy spread, shortened beam lifetime or bunch-to-bunch jitter of the beam orbit or of the bunch arrival time. Examples of mechanisms that can affect the beam lifetime are the transverse mode-coupling instability and multi-bunch coupling. The first phenomenon is single-bunch, the second multi-bunch. In the coupled-bunch instability, all the bunches act together in such a way as to cause a resonance whose typical time scale is quite short. Therefore, unless a feedback system is active, a coupled-bunch instability can lead to sudden beam losses. An example of instability that degrades the beam quality is the longitudinal microwave instability, which increases the energy spread and the

bunch length. Longitudinal multibunch oscillations can be stable (finite amplitude oscillations), but they cause a jitter in the arrival time of the bunches at a given point in the machine, thus having a detrimental effect on applications that are sensitive to time resolution. Similarly, stable transverse multibunch oscillations lead to an effective increase in the beam emittance and hence a degradation of the brightness of the emitted synchrotron light.

12.1.3 Damping Mechanisms

The most important way to mitigate single-bunch instabilities is by careful design of the vacuum chamber. Modern designs place a premium on its smoothness, since this leads to smaller impedance and hence a decreased chance for instabilities at a given bunch current. In practice, of course, it is not possible to have a perfectly smooth chamber, and hence certain compromises must be made.

Two mechanisms that help damp instabilities exist naturally in any electron storage ring. The first and most obvious one is the damping provided by the radiation of the synchrotron light. Instabilities whose growth time is longer than the damping time (which is typically on the order of several thousand turns), do not manifest themselves as such and do not lead to a problem. The second mechanism, which is more subtle, is Landau damping. As explained in more detail below, this mechanism requires a spread in the oscillation frequency of the particles within a bunch. Landau damping effectively transforms the coherent motion of the beam into incoherent motion of the particles via phase mixing induced by the oscillation frequency spread. In the case of transverse oscillations, a frequency spread is provided naturally by the unavoidable machine nonlinearities which, in turn, lead to an amplitude dependence of the betatron frequencies. A longitudinal frequency spread also exists naturally due to the sinusoidal RF voltage, leading to nonlinearity of the synchrotron forces at large amplitude. If the natural nonlinearities are not strong enough (in the case of small-emittance beams, for example), there are artificial means of enhancing them, as discussed below.

In any case, these damping mechanisms are typically not enough to eliminate all instabilities in modern light sources, at least not when these machines are operated in high-current, multi-bunch mode. Certain instabilities can be avoided by proper choice of parameters; for example, the Robinson instability is avoided by a slight detuning of the fundamental RF frequency away from $h\omega_0$, where h is the harmonic number (see Chapter 4) and ω_0 is the angular revolution frequency.

Generally speaking, the design of most synchrotron light sources is such that single-bunch instabilities are avoided, or at least are not serious. Coupled-bunch instabilities are alleviated by damping the HOMs of the RF cavities, which can be achieved by clever design of the cavity shape, and by adding damping elements. However, it is typically impossible to avoid all such instabilities by passive methods. An active feedback system (see Chapter 13) is thus required that detects incipient unstable motion and applies appropriate compensating time-dependent forces to counteract it. Although it is in principle possible to design a feedback system that would eliminate single-

bunch instabilities, in practice the power and bandwidth requirements on such a system would typically make it prohibitively expensive.

12.2 Wake Fields and Impedances

12.2.1 Definitions[2]

Whenever a relativistic charged particle travels near a material that is not perfectly smooth or not perfectly conducting, an electromagnetic field is created that extends for a certain distance behind it and lasts for a certain characteristic time before it dissipates. This is the *wake field* which, in turn, can act back on the particles traveling behind the one that created it. If the wake field lasts for a sufficiently long time, it will affect the particles in trailing bunches in successive turns. The impedance is essentially the Fourier transform of the Lorentz force caused by the wake field, and is thus a measure of the strength and shape of the frequency spectrum of this time-varying force

In the simplest version, the "beam" consists of a single particle of charge q traveling at the speed of light c down a cylindrically-symmetric pipe. The beam trajectory is a straight line parallel to the axis but is offset transversely from it by $\mathbf{x}$. We consider a "test particle" of charge e also traveling at the speed of light parallel to the beam at a distance z behind it, with some transverse position of its own. The pipe need not be perfectly conducting or smooth; however, we assume that the lack of smoothness is not extreme, and the average pipe radius is b. From Maxwell's equations one can calculate in principle the transverse and longitudinal electromagnetic force on the test particle. If we integrate these forces over a distance $L \gg b$, we obtain, by definition, the *wake functions* $W_{\|}(z)$ and $W_{\perp}(z)$

$$\int_0^L ds\, F_{\|} \equiv -eqW_{\|}(z) + \cdots, \qquad \int_0^L ds\, \mathbf{F}_{\perp} \equiv -eq\mathbf{x}W_{\perp}(z) + \cdots \tag{12.1}$$

where $\cdots$ refers to terms of higher order in $\mathbf{x}$ and in the transverse position of the test particle, and where the integration variable s is the distance along the trajectory of the test particle. The corresponding impedances for the distance L are defined by the Fourier transform of the wake functions, and are given by

$$Z_{\|}(\omega) \equiv \frac{1}{c}\int_{-\infty}^{\infty} dz\, e^{-i\omega z/c}\, W_{\|}(z), \qquad Z_{\perp}(\omega) \equiv \frac{i}{c}\int_{-\infty}^{\infty} dz\, e^{-i\omega z/c}\, W_{\perp}(z) \tag{12.2}$$

where the sign convention is that $z < 0$ means that the test particle is *behind* the beam.

Obviously, the distinction between the beam and the test particle is a purely mathematical one that allows one to define wake functions and impedances. In a real machine, all particles play both roles, since they produce wake fields and are, in turn, affected by the wake fields of all particles.

Impedances summarize all the electromagnetic effects from the environment traversed by the beam. Thus the vacuum chamber resistivity, RF cavities, bellows, discontinuities, vacuum ports,

flanges, curvature of the chamber, synchrotron radiation reaction, etc., all contribute to the impedance. For a circular machine, the distance L in (12.1) is usually taken to be the circumference, so that Eqs. (12.2) represent the whole-ring impedances. In reality, the forces on the test particle fluctuate as the beam and the test particle traverse the different structures along the vacuum chamber. A basic underlying assumption in the usefulness of the wake functions is that the forces on the test particle do not deviate much from their average value. In some cases, however, this averaging does not yield accurate results for certain instabilities such as those caused by coherent synchro-betatron resonances.[3] In these cases, the localized nature of the impedance is important and special methods, such as simulation codes with a time-dependent Maxwell's equations solver, must be used; we will not be concerned with such a possibility here. Therefore, even though wake functions are defined in principle for arbitrary boundary conditions, their usefulness as analytical tools diminishes as the characteristics of the vacuum chamber become more and more complicated. Fortunately most modern accelerators do not fall under this category.

Even for a point charge in a perfectly smooth cylindrical pipe, there is an infinite number of wake functions (and impedances) represented by ⋯ in Eq. (12.1). These terms represent a power-series expansion of the transverse or longitudinal force in the transverse displacement of the beam and of the test particle. The leading terms are those shown above, namely the monopole longitudinal wake function, usually labeled $m = 0$, and the dipole transverse wake function, usually labeled $m = 1$. The corresponding impedances $Z_{\parallel}(\omega)$ and $Z_{\perp}(\omega)$ in Eqs. (12.2) are also labeled $m = 0$ and $m = 1$, respectively. The words "monopole" and "dipole" refer to the fact that the forces are produced by the monopole and dipole moments of the charge distribution of the beam, respectively (note that the forces on the test particle, Eqs. (12.1), are independent of its transverse position through dipole order). The higher-order impedances become important when the transverse size of the beam is comparable to the vacuum pipe diameter. We shall not be concerned here with any m's higher than 1 for the transverse case or higher than 0 for the longitudinal (the transverse $m = 0$ wake function vanishes by symmetry), and we will omit the label m.

On the other hand, the *longitudinal* charge distribution does matter in many cases. Thus, for most purposes, we can view the beam as consisting of needle-like bunches, and the calculation of the electromagnetic force on the test particles requires a superposition over the longitudinal charge distribution, typically assumed Gaussian. The impedance resulting from this superposition is called the *effective impedance*.

12.2.2 Properties and Basic Uses of Impedances[2]

As implied by Eqs. (12.1), the wake functions are *real functions*. Therefore, by taking the complex conjugate of Eqs. (12.2) we conclude that $Z_{\parallel}(\omega)^* = Z_{\parallel}(-\omega)$ and $Z_{\perp}(\omega)^* = -Z_{\perp}(-\omega)$. Therefore the real part of $Z_{\parallel}(\omega)$ is a symmetric function of ω, while the imaginary part is antisymmetric; the transverse impedance $Z_{\perp}(\omega)$ has the opposite parity properties, on account of the extra factor of i in its definition. These parity properties are generic of all impedances, not just

those defined above.

Another generic property of the wake functions is that they are *causal functions*: since the forces ahead of the beam vanish, any wake function satisfies

$$W(z) = 0 \quad \text{for } z > 0. \tag{12.3}$$

A fundamental theorem of the Fourier transform of causal functions then implies that the corresponding impedance is an analytic function in the upper half of the complex-ω plane. One consequence of this is that the impedances satisfy a *dispersion relation* that relates the real and the imaginary parts: if the real part is known for all frequencies, the imaginary part is uniquely determined from the dispersion relation and vice versa. As a by-product of the dispersion relation, one concludes that any impedance must satisfy

$$Z(\omega) \to 0 \ \text{ as } \omega \to \pm\infty. \tag{12.4}$$

Even though there is no generally-valid relation between longitudinal and transverse impedances of different *m*'s, qualitative arguments[2] show that the $m = 0$ longitudinal and the $m = 1$ transverse impedances are related by

$$Z_\perp(\omega) \approx \frac{2c}{b^2\omega} Z_\parallel(\omega) \tag{12.5}$$

This relation is strictly valid for the resistive wall impedance of a smooth, infinitely long, cylindrical pipe of radius *b*. It is approximately valid for other impedances arising from discontinuities in the chamber wall such as bellows, small cavity-like structures or other objects, provided their characteristic size is small compared to *b*. For larger objects, such as RF cavities, Eq. (12.5) is valid in an average sense, although it becomes more accurate at frequencies above the cut-off frequency ω_c, defined below.

In calculating beam instabilities, the longitudinal impedance usually appears divided by ω. Therefore, instead of $Z_\parallel(\omega)$, it is customary to deal with the quantity $Z_\parallel(\omega)/n$, where *n* is defined by $n \equiv \omega/\omega_0$. Thus $Z_\parallel(\omega)/n$ has the opposite parity properties as $Z_\parallel(\omega)$, and the approximate relation (12.5) reads

$$Z_\perp(\omega) \approx \frac{2R}{b^2} \frac{Z_\parallel(\omega)}{n} \tag{12.6}$$

where *R* is the average radius of the accelerator.

Equations (12.2) imply that $Z_\parallel(\omega)$ (and hence $Z_\parallel(\omega)/n$) is measured in Ω while $Z_\perp(\omega)$ is measured in Ω/m. Modern storage rings, whether colliders or light sources, are typically designed for operation in high-current, multibunch mode. Stable operation requires that the impedance should be kept small, which implies the need for a smooth vacuum chamber. Typically, the *broad-band average* (defined below) of the impedance for these modern rings is $\left|Z_\parallel/n\right|_{bb} \approx 0.1 - 2\ \Omega$. Older rings, which were not designed with these requirements in mind, typically have longitudinal

impedance values $\left|Z_{\|}/n\right|_{bb}$ in the range one to tens of Ω. Figure 12.2 shows a photograph of a joint in the injection region of the ALS vacuum chamber that exemplifies the attention paid to keeping the impedance low.

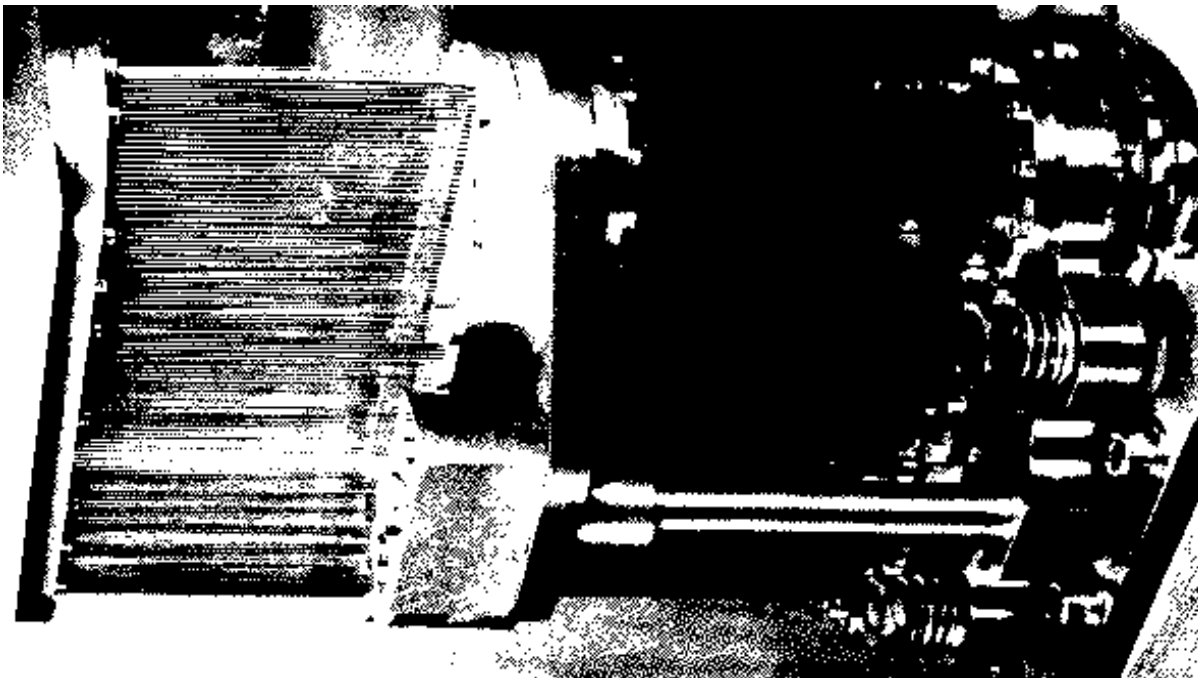

Fig. 12.2. A transition joint in the vacuum chamber in the injection region of the ALS. The joint must be flexible in order to accommodate a transverse motion of a few cm during injection. The required flexibility and low impedance is achieved by a "wire cage" design (the entire assembly shown is enclosed in a large bellows in order to maintain the vacuum). If the joint had been left open, the discontinuity would have led to a large impedance. Photo courtesy of J. Corlett.

The integral that defines the longitudinal wake function in Eq. (12.1) is also equal to the change of energy of the test particle in the distance L due to the wake fields, so that

$$\Delta E = -eqW_{\|}(z) \tag{12.7}$$

(the sign convention is that $\Delta E > 0$ means that the test particle gains energy). For a bunch of particles, the total energy change in the distance L is given by a superposition over its longitudinal charge distribution $\rho(z)$. Assuming that the bunch length and the range of the wake function are both $\ll L$ one obtains[a]

[a] If the bunch length or the range of the wake function are not small, the integral in this equation must be replaced by a summation over the harmonics of the bunch frequency.

$$\Delta E = -\int_{-\infty}^{\infty} \frac{d\omega}{2\pi} \left|\tilde{\rho}(\omega)\right|^2 \operatorname{Re} Z_{\|}(\omega) \tag{12.8}$$

where $\tilde{\rho}(\omega)$ is the Fourier transform of $\rho(z)$. Only the real part of the impedance contributes to the integral because $\left|\tilde{\rho}(\omega)\right|$ is an even function of ω (this follows from the fact that $\rho(z)$ is real). Since the beam as a whole can only lose energy, and this must be true for an arbitrary charge distribution, it follows that

$$\operatorname{Re} Z_{\|}(\omega) \geq 0 \quad \text{for all } \omega. \tag{12.9}$$

The energy loss of a bunch is often expressed in terms of the *loss parameter* (or *loss factor*) *k*, which is defined to be

$$k = -\Delta E / q^2 \tag{12.10}$$

where ΔE and q are here the total energy change and the total charge of the bunch, respectively. The loss parameter is always positive, and its typical numerical value for RF cavities is ~a few V/pC. In practice, the bunch-length dependence of the loss parameter can give useful information about the impedance of cavities or cavity-like objects.

Equation (12.1) allows one to define an impedance-induced voltage which is the potential energy change of the test particle in the distance *L* due to the wake field. For a beam described by a charge distribution $\rho(z)$, this potential energy change is given by

$$V_{\|}(z') = -\int_{-\infty}^{\infty} dz\, \rho(z)\, W_{\|}(z' - z) \tag{12.11}$$

where we make the same assumptions as in the derivation of Eq. (12.1). In the frequency domain this equation is usually written

$$\tilde{V}_{\|}(\omega) = -\tilde{I}(\omega) Z_{\|}(\omega) \tag{12.12}$$

where $\tilde{I}(\omega)$ is the Fourier transform of the current, defined by $I(z) = c\rho(z)$.

12.2.3 Resonator Impedance Model

In practice it is impossible to accurately know the impedances for the ring as a whole. However, impedances of individual components can often be calculated or measured at least in a certain frequency range. More typically, one resorts to simple models with a few parameters for a given ring component; the parameters are then determined by fitting the model to the measurements. A simple and widely-used model for the longitudinal impedance of a resonant structure such as an RF cavity is the superposition

$$Z_{\parallel}(\omega) = \sum_r Z_{\parallel,r}(\omega) \tag{12.13}$$

where $Z_{\parallel,r}(\omega)$ is a *single-resonator impedance*, defined by

$$Z_{\parallel,r}(\omega) = \frac{R_{S,r}}{1 + iQ_r\left(\frac{\omega_r}{\omega} - \frac{\omega}{\omega_r}\right)}. \tag{12.14}$$

Here Q_r is the *quality factor*, ω_r is the (angular) *resonant frequency*, and $R_{S,r}$ is the strength of the resonator, or *shunt impedance* (measured in Ω). Eq. (12.5) allows one to define a transverse resonator impedance which is of the same form as Eq. (12.14) except for an additional overall ω^{-1} factor.

The real part of the resonator impedance $Z_{\parallel,r}(\omega)$ has peaks at $\omega \approx \pm\omega_r$ with FWHM$= \omega_r / Q_r$. The imaginary part changes sign as the frequency crosses its resonant value. By definition, a *broad-band resonator* has a relatively low Q, typically $Q \approx 1$, and therefore wide peaks. A *narrow-band resonator* has large Q and hence narrow peaks. For example, the typical resonant modes of ordinary RF cavities have Q's of order $10^2 - 10^4$, while those of superconducting cavities have Q's of order $10^6 - 10^9$. By taking the Fourier transform of (12.14) one finds that the decay time of the excitation produced by a resonator is $\tau_r = 2Q_r/\omega_r$. Therefore, narrow resonances last for a long time and thus are a leading cause of coupled-bunch instabilities.

The real part of any impedance is called the *resistive component* while the imaginary part is the *reactive component*. As shown above, only the resistive component can dissipate energy. If the reactive part is positive, it is called *capacitive*; if negative, *inductive*.[b] This terminology arises from the fact that a pure inductor L has an impedance $Z = -i\omega L$, which is negative imaginary, while a pure capacitor C has an impedance $Z = i/\omega C$, i.e., positive imaginary. In fact, a simple model for the single-resonator impedance is an RLC circuit in which all three elements are in parallel, and

[b] Many authors define the impedance with i replaced by $-j$ in Eqs. (12.2). This can lead to confusion in the definitions of capacitive and inductive. Whatever convention is used, the defining condition for a capacitive impedance is that the response is ahead of the excitation, while for an inductive impedance the response lags in phase behind the excitation.

where the resistance is R_S. In this model the impedance is given by $Z^{-1} = R_S^{-1} + i/\omega L - i\omega C$ which is precisely of the same form as Eq. (12.14). The resonant frequency and the quality factor are given by $\omega_r = 1/\sqrt{LC}$ and $Q_r = R_S\sqrt{C/L}$, respectively.

For a broad-band resonator with $Q = 1$, the reactive part of $Z_{\|,r}(\omega)/n$ is inductive and almost independent of frequency in the range $-\omega_r \lesssim \omega \lesssim \omega_r$, while the resistive part has an approximately linear frequency dependence in this range. These properties are also true of $Z_\perp(\omega)$ on account of Eq. (12.6).

The loss factor for a high-Q resonator impedance ($Q \gg \sigma_t\omega_r$) traversed by a Gaussian bunch with rms bunch length σ_t (in time units) follows from Eq. (12.8),

$$k = \frac{R_{S,r}\omega_r}{2Q_r} e^{-(\sigma_t\omega_r)^2}. \tag{12.15}$$

Typically, the fundamental mode of a cavity has the lowest frequency, and is labeled by $r = 0$; this is typically the TM_{010} mode used to accelerate the particles or to replenish their energy that has been lost by the radiation process (see Chapter 4). HOMs, also called parasitic modes, are usually undesirable but unavoidable. Ideally, the Q's should be large for $r = 0$ and small for $r \geq 1$. In practice, one tries to reduce the Q's of the HOMs as much as possible by cleverly reshaping the cavity or adding dampers. This is called "de-Qing," or damping, the modes. Typically, it is impossible to de-Q all the HOMs to the point that coupled-bunch instabilities are absent, hence the need for a feedback system. A prototype RF cavity for the PEP-II collider is shown in Fig. 12.3, which exhibits the three wave guides used to damp many HOMs.

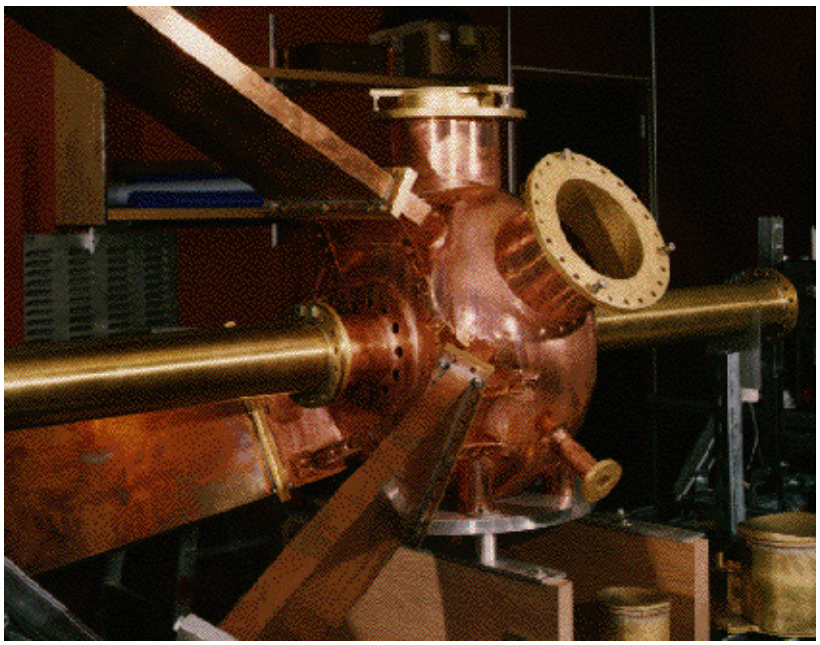

Fig. 12.3. Prototype of the PEP-II collider cavity. The three large rectangular wave guides emanating from the body of the cavity are terminated with ferrite, and are used to damp the HOMs. Photo courtesy of R. Rimmer.

12.2.4 Impedance Beyond Cutoff[4]

If an RF cavity (or any cavity-like structure) were closed it would have an infinite number of modes. In practice, there are at least two openings needed for the beam traversal. Therefore, those modes whose wavelength is smaller than the pipe radius are not trapped in the cavity and are not resonant. Thus there is a natural *cutoff frequency*, ω_c, above which there are no more resonant cavity modes. It is usually defined by[c]

$$\omega_c \equiv c/b \tag{12.16}$$

In modern storage rings and light sources there is an increasing demand for shorter and shorter bunch lengths. The shorter the bunch, the higher the reach of its frequency spectrum. If the bunch is short compared to the vacuum pipe radius, its frequency spectrum reaches beyond the cutoff frequency. Therefore the behavior of the impedance at these high frequencies can become important and needs to be examined.

The source of impedance beyond cutoff is the interaction of the beam with the synchrotron radiation that propagates down the vacuum chamber which, in turn, interacts with the different structures in the chamber. In addition, the curvature of the trajectory can make particles resonate with waves having the same angular phase velocity as the particles.

The high-frequency impedance of a curved toroidal vacuum chamber can be understood simply in terms of the far-field radiation in free space of a particle beam on a curved trajectory. Synchrotron radiation along a curved trajectory provides a dissipative mechanism analogous to resistive wall effects. The radiation reaction force follows from a longitudinal self-field that extracts kinetic energy. Neglecting the shielding provided by the vacuum chamber, the resultant *free space impedance* is given by

$$Z_{\|}(\omega)/n = \frac{\frac{1}{2}\Gamma\left(\frac{2}{3}\right)}{(3n^2)^{1/3}}\left(\sqrt{3}-i\right)Z_0 \tag{12.17}$$

where $\Gamma(2/3) \approx 1.35$ is the gamma function and $Z_0 = 4\pi/c \approx 377\ \Omega$ is the so-called *vacuum impedance*. This formula is valid for frequencies below the critical frequency (see Chapter 1), given by $\omega_{\rm crit}/\omega_0 = 3\gamma^3/2$ where γ is the usual relativistic factor of the particle (for $\omega > \omega_{\rm crit}$ the impedance falls off exponentially). The $n^{1/3}$-dependence of $Z_{\|}(\omega)$ is a consequence of the well-known $\omega^{1/3}$-dependence of the synchrotron radiation power at large frequency of a particle in circular motion. The real part of the free space impedance has the approximate numerical value

$$\mathrm{Re}\, Z_{\|}(\omega) \approx 300\ n^{1/3}\ \ \Omega. \tag{12.18}$$

The beam pipe, however, provides shielding for low frequencies: radiation is essentially suppressed for harmonics below a cutoff given by $n_c \approx (R/b)^{3/2}$. This expression for n_c is exact

[c] For a perfect cylindrical pipe the cutoff frequency is $2.405c/b$. Since, in practice, the geometry is much more complicated, the usual convention is to choose the numerical factor to be unity for simplicity.

for a planar circular trajectory between two infinite conducting planes parallel to the orbit plane. As a result of this shielding, the maximum free space impedance is then given by

$$\left|\frac{Z_{\|}(\omega)}{n}\right|_{\max} \approx 300\, n_c^{-2/3}\ \ \Omega = 300\left(\frac{b}{R}\right)\ \Omega . \tag{12.19}$$

This result happens to be approximately the same for a large class of shielding geometries. Since, typically, $b/R = O(10^{-4})$, this means that the shielded free space value of $|Z_{\|}/n|$ is rather small. Nevertheless, prudent ring designers typically assume Eq. (12.19) to provide a *lower* bound for the estimate of the impedance beyond cutoff.

For vacuum chambers with cavity-like structures, several models have led to the generic behavior $Z_{\|}(\omega) \propto \omega^{-p}$ for the longitudinal impedance at high frequency. A crucial distinction has been established between a single isolated structure and an infinitely long sequence of cavities: for the first case, the power p has been found to be $p = 1/2$ while for the second, $p = 3/2$.

12.2.5 Impedance Calculations and Measurement Techniques[5]

The modeling and calculation of storage ring impedances has vastly improved over the past 20 years, mostly due to increased computer power and improved algorithms for the solution of Maxwell's equations. For example, electromagnetic modeling codes such as MAFIA[6] can calculate, in principle, the wake function and impedance of any three-dimensional geometry. In practice, if the geometry of the object is sufficiently complicated, the calculations become limited by the power of the computer used to run the codes.

Several bench impedance measurement techniques are used for testing actual or prototype beamline components. For nonresonant components, a wire is passed on axis and the transmission through it is measured as a function of frequency. For resonant structures, the strength of a mode is found by exciting it and measuring the resulting field pattern along the beam axis by introducing a small movable perturbing needle. The frequencies and quality factors of the resonant modes are found by measuring the transmission through the structure. Electromagnetic codes calculate quite accurately the R/Q ratios; by combining these calculated values with the measured Q's one can extract accurate values for the shunt impedances.

The impedance of individual resonant modes with $Q \gtrsim 10$ can be measured by the frequency-perturbation method. This is done by using beads or needles which shift the resonant frequency. From this one can measure the energy density on resonance and extract the R/Q ratios. In practice, since the dimensions of the perturbing object must be much smaller than the wavelength of interest, this technique cannot be used reliably at high frequency.

The pulsed-beam method is conceptually the most attractive since it closely mimics the dynamics in the storage ring, and the definition of the wake field given by Eq. (12.1). This method consists of passing a pulse of electrons through the test object and measuring the energy loss or the deflection of the trajectory to get the real part of $Z_{\|}$ or $Z_{\perp}$. To obtain the full wake function, one can

use a smaller "witness" beam to sense the delayed effects. One can also probe with antennas to study the excitation in the test object. The Wake Field Test Facility at ANL is devoted to this method.[7]

Finally, of course, measurement of instability thresholds, bunch lengthening, etc., in operating storage rings may be the ultimate phenomenological tool to check calculations, predict behavior and evaluate cures. From these measurements one can, in principle, extract the ring impedance if the models used in the calculations are sufficiently complete and the measurements sufficiently accurate.

12.2.6 Broad-Band Impedance Model

In spite of the progress in the calculation and measurement of the impedance of individual components, the determination of the impedance of the storage ring as a whole is a challenging and typically imperfect task. Even more challenging is the calculation of the net effect on the beam given the individual component impedances. Experience has led to the development of the so-called *broad-band impedance model* to account for the entire storage ring impedance. This model provides a simple conceptual and calculational tool and it adequately represents a wide variety of storage rings. It has been particularly successful in describing the beam behavior in storage rings with longer bunches. Machine design reports usually contain an "impedance budget" listing the contributions of the different ring components to the impedance. In its simplest version, the longitudinal broad-band impedance model of the ring has three components:

- A broad-band resonator with ω_r and Q typically chosen to be $\omega_r \approx \omega_c$ and $Q \approx 1$. The shunt impedance R_{bb} is determined empirically from a fit to the data. This broad-band resonator accounts for the impedance contribution of all vacuum chamber components such as bellows, joints, low-Q parasitic cavity modes, vacuum chamber discontinuities, etc.
- A low-frequency contribution from the skin effect of the vacuum chamber known as the *resistive wall impedance*.
- Various narrowband resonator impedances including the fundamental mode of the RF cavity and other parasitic cavity modes.[d]

The contribution from the resistive wall impedance can be easily estimated for a typical vacuum chamber. For all frequencies of practical interest, the longitudinal impedance per unit length for an infinite cylindrical pipe of radius b is given by[e]

$$Z_{\|}(\omega)/L = \frac{Z_0}{4\pi b}(1 - i\varepsilon(\omega))\frac{\delta(\omega)|\omega|}{c} \tag{12.20}$$

where $\varepsilon(\omega)$ is the sign function, $\delta(\omega) = c\sqrt{2\pi\sigma|\omega|}$ is the skin depth of the vacuum chamber whose conductivity is σ.

[d] Many authors exclude these narrowband components from the definition of the broadband impedance model.
[e] This formula is not valid for frequencies so low that the skin depth is comparable to or larger than the thickness of the vacuum pipe. It is also not valid at extremely high frequencies.

Determination of R_{bb} involves a wide variety of components. This shunt impedance is conventionally quoted as $\left|Z_{\|}/n\right|_{bb}$, which is defined to be

$$\left|\frac{Z_{\|}}{n}\right|_{bb} \equiv \lim_{\omega\to 0}\left|\frac{Z_{\|}(\omega)}{n}\right| = \frac{R_{bb}\omega_0}{Q\omega_r} \tag{12.21}$$

whose typical value for modern storage rings is in the range $\left|Z_{\|}/n\right|_{bb} = 0.1-1\,\Omega$. For illustrative purposes we sketch the broad-band impedance for a hypothetical storage ring in Fig. 12.4.

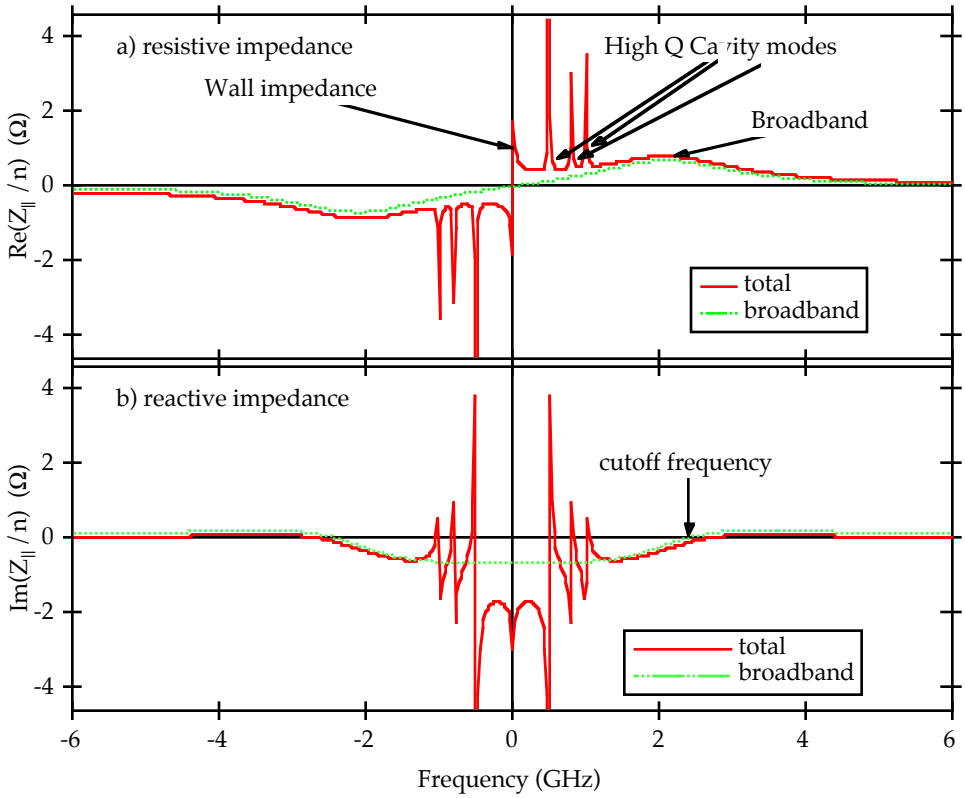

Fig. 12.4. Sketch of the broad-band impedance for a hypothetical ring. The value of $\left|Z_{\|}/n\right|_{bb}$ relative to the shunt impedance of the narrowband resonators has been highly exaggerated.

12.3 Landau Damping

As mentioned earlier, the synchrotron radiation provides natural damping: if the growth time of an instability is larger than the damping time of the ring, obviously it fails to materialize. A second damping mechanism, called Landau damping, is more subtle but just as important, and we sketch here the basic physics underlying it. This mechanism requires a *spread* in the oscillation frequency, or tune, of the particles.[8,9,2]

Consider a single particle executing transverse or longitudinal motion at low amplitude. The particle creates a wake field that acts back on itself, driving it on resonance and leading to an instability. This simple picture would lead one to expect essentially all particle motion in an accelerator to be unstable. Landau damping is one of the reasons why, in practice, this expectation is

pessimistic.

Concretely, consider a single harmonic oscillator subject to a time-dependent sinusoidal force. The equation of motion is

$$\ddot{x} + \omega^2 x = A\cos\Omega t \tag{12.22}$$

and we assume that the initial conditions are $x(0) = \dot{x}(0) = 0$. If the force drives the particle resonantly, i.e., if $\Omega = \omega$, then the amplitude of the motion grows indefinitely according to

$$x(t) \propto At\sin\Omega t. \tag{12.23}$$

Correspondingly its energy, which is proportional to $\langle x^2 \rangle$, grows like $\sim t^2$ for large *t*. implying instability.

An *ensemble* of particles (such as a bunch), however, can behave in a qualitatively different fashion *even if the particles do not interact among themselves*, provided their natural oscillation frequencies are spread over a certain range. Thus we assume that the oscillators have a narrow frequency spectrum $\rho(\omega)$ of width $\Delta\omega$, and that they are all driven by the same force, $F = A\cos\Omega t$, where Ω lies within the range of $\rho(\omega)$. For times $t \gg 1/\Delta\omega$ one finds that the centroid of the ensemble is given by

$$\langle x \rangle \propto A\left[\cos\Omega t\ \mathrm{P}\int d\omega \frac{\rho(\omega)}{\omega - \Omega} + \pi\rho(\Omega)\sin\Omega t\right] \tag{12.24}$$

where the symbol "P" instructs one to take the principal value of the integral at the singularity and the spectrum is normalized such that $\int d\omega\, \rho(\omega) = 1$. One also finds that the energy of the bunch grows in time like

$$\langle x^2 \rangle \propto A^2 t\rho(\Omega)\cdot \tag{12.25}$$

The ensemble case and the single-particle case behave qualitatively differently in that the power of *t* with which the amplitude and the energy grow is one less in the former than in the latter. This is the essence of Landau damping: the energy pumped into a bunch of particles goes into increasing its size rather than the amplitude of the motion of the centroid. In most practical cases, this increase in bunch size does not present a problem, and therefore the instability is avoided.

If the oscillators are finite in number and their frequencies take on discrete values over the range $\Delta\omega$, Landau damping works qualitatively in the same way as for the continuum case, except for one difference: the mechanism ceases after a time $\sim 1/\delta\omega$, where $\delta\omega$ is the minimum frequency spacing between the oscillators in the ensemble. The explanation is that, the system being conservative, the driving force and the oscillators exchange energy back and forth in a beating pattern whose period is $\sim 1/\delta\omega$ (we assume that none of the oscillators is exactly on resonance). Therefore, after this time, the ensemble of oscillators comes back to its initial state and the process starts again. For a uniform distribution of *N* oscillators, $\delta\omega = \Delta\omega/N$. Therefore, for a given finite *N*, this consideration puts a constraint on how wide $\Delta\omega$ can be for Landau damping to be practical.

For a bunch of *N* particles, one expects $\delta\omega \approx \Delta\omega/N$ and so the damping ceases after a time

$\sim N/\Delta\omega$. In practice, however, since $N \sim 10^{11}$, this constraint is not significant unless the frequency spread $\Delta\omega$ is very large. On the other hand, if $\Delta\omega$ is too small, the long-time limit (12.24) is effectively never reached, and the mechanism does not take effect. The energy is not stored evenly within the bunch: it is selectively stored in particles with a continuously narrowing range of frequencies ω near Ω. The energy stored in these particles grows like t^2, but there are fewer and fewer of them as time progresses. If the driving frequency Ω falls outside the range of $\rho(\omega)$, damping clearly does not take effect and the instability is not avoided.

The analysis for a realistic case is more complicated than what is sketched above because the amplitude *A* of the driving force in Eq. (12.22) is itself proportional to the bunch centroid $\langle x \rangle$. Furthermore, the force is a superposition of all wake forces from all turns prior to time *t*. Either one of these two facts imply that the $\cos\Omega t$ and $\sin\Omega t$ terms in Eq. (12.24) get mixed because the force is out of phase with $x(t)$. In the frequency domain, this mixing is a consequence of the complex nature of the impedance. The fact that the driving force is proportional to $\langle x \rangle$ implies that a *consistency condition* must be satisfied by the solution. This condition takes the form of a *dispersion relation*. For transverse motion of a single bunch, we look for a solution of the form $x \propto \langle x \rangle \exp(-i\Omega t)$, in which case the dispersion relation reads

$$1 = i \frac{N c r_e \bar{Z}_\perp}{2\gamma \omega_\beta T_0^2} \int d\omega \frac{\rho(\omega)}{\omega - \Omega - i\varepsilon} \tag{12.26}$$

where $r_e = e^2/m_e c^2 \approx 2.82 \times 10^{-15}$ m is the classical electron radius, γ is the usual relativistic factor, T_0 is the revolution period, ε is a small number whose limit $\varepsilon \to 0^+$ is to be taken after the integral is done, and $\bar{Z}_\perp$ is defined by

$$\bar{Z}_\perp = \sum_{p=-\infty}^{\infty} Z_\perp(p\omega_0 + \omega_\beta) \tag{12.27}$$

where the summation is over all integers. In general, the solution for Ω is complex. In practice, Eq. (12.26) is used as follows: one assumes a certain form for $\rho(\omega)$ (say a Gaussian), and one lets Ω vary in the range $(-\infty, \infty)$ through the real numbers. Then $\bar{Z}_\perp$ obtained from (12.26) traces out a line in the complex plane that divides it into two regions. Since Ω is assumed to be real, this line defines a *stability boundary*. On either side of this boundary, Ω has a nonzero imaginary part. If the actual value of $\bar{Z}_\perp$ of the machine lies in the region containing the origin of the complex plane, then $\mathrm{Im}\,\Omega < 0$ and the motion is stable, i.e., it is Landau damped. If $\bar{Z}_\perp$ lies in the other region, then $\mathrm{Im}\,\Omega > 0$ and the motion grows exponentially in time (it is said to be "antidamped"), and an instability materializes if $\mathrm{Im}\,\Omega$ is larger than the damping time of the machine. Therefore, by making several reasonable assumptions about $\rho(\omega)$, one gets an approximate criterion for the allowed values of $\bar{Z}_\perp$ that lead to stability. Note that this method establishes a stability criterion for $\bar{Z}_\perp$ and not for the impedance itself.

For modern storage rings, the main constraint on the practicality of Landau damping is that

the spectrum width $\Delta\omega$ is too narrow. A transverse tune spread is provided naturally by the magnet nonlinearities which produce an amplitude dependence of the betatron tune. A longitudinal tune spread is provided by the nonlinearity of the synchrotron forces at large amplitude. However, modern light sources have small emittances and short bunch lengths, and therefore the natural motion of the particles is very linear. As a result, the naturally-existing nonlinearities may not be strong enough to produce an appreciable tune spread. If this is the case, there are means of enhancing the nonlinearities: for transverse motion, one can add octupole magnets; for longitudinal motion, one can add a low-power harmonic RF system that effectively distorts the harmonic-oscillator shape near the center of the RF bucket. Obviously, a delicate compromise is needed in these cases because nonlinearities introduce single-particle resonances or chaotic motion that tend to degrade the beam lifetime.

12.4 Single-Bunch Issues[10]

Single bunch collective phenomena arise from the interaction of a bunch with itself via wake fields whose range is comparable to or shorter than the bunch length. The most ubiquitous single-bunch effect is the so-called *longitudinal microwave instability*, or *turbulent bunch lengthening instability*. This instability does not grow indefinitely: if the beam current is large enough that this instability is excited, the bunch length and energy spread increase until a new equilibrium situation is reached. In the transverse plane, the instability that, typically, has lowest threshold, is the *transverse mode-coupling instability*, or *fast head-tail instability*. This instability leads to fast beam loss; however, the current threshold is typically higher than for the microwave instability, and is easily avoidable.

12.4.1 Calculation of Instabilities

The calculation of thresholds and growth rates of instabilities and other collective effects is codified in codes such as ZAP.[11] A rough sketch of the procedure, applicable to most instabilities (single bunch and multi bunch), is as follows: one first assumes that the low-amplitude particle motion (transverse or longitudinal) corresponds to a simple harmonic oscillator. One then adds the extra force produced by the wake field, and solves for the frequency in lowest-order approximation. For example, the horizontal equation of motion at turn n for a single particle reads

$$x_n'' + (\omega_\beta / c)^2 x_n = \text{const.} \times \sum_{k=-\infty}^{n} W(-kL) x_k \tag{12.28}$$

where the summation over the transverse dipole wake function W represents the superposition of the force from all turns prior to n, ω_β is the betatron frequency, L is the ring circumference, and the primes mean derivatives with respect to the azimuthal position s. By substituting $x_n = A\exp(-is\Omega/c)$, one can solve for the frequency Ω in lowest-order approximation in the impedance.

The real part of Ω implies a frequency shift, which is not in itself detrimental. The imaginary

part, however, signals a potential instability whose lifetime τ is given by

$$\tau^{-1} = \mathrm{Im}\,\Omega. \tag{12.29}$$

If $\tau < 0$, the disturbance is damped and does not lead to any problems. But if $\tau > 0$ the disturbance is antidamped and potentially unstable. However, one cannot conclude from this analysis that the disturbance grows indefinitely because other forces may become important at large amplitude that stop it from growing further; this is precisely what happens in the longitudinal microwave instability.

12.4.2 Parasitic Power Loss

As mentioned earlier, the beam image currents dissipate energy into the vacuum chamber components in addition to generating wake fields. This is referred to as parasitic loss, and the dissipated power is proportional to the square of the bunch current. Although this power loss does not inherently affect the beam stability, it can effectively limit the bunch current (and hence the total beam current) because of the excessive heating of the vacuum chamber. This problem usually affects imperfect junctures in the vacuum chamber such as bellows.

For a beam consisting of *M* identical bunches, one can generally write the power loss for the whole beam in the form

$$P = M I_b^2 Z_{\mathrm{loss}} \tag{12.30}$$

where the bunch current I_b is related to the total beam current I_0 via $I_0 = MI_b$, and where the *loss impedance* Z_{loss} is nothing but the real part of the effective impedance that is causing the energy loss (Z_{loss}, of course, is proportional to the loss factor). We are only concerned here with Gaussian bunches whose rms bunch length is σ_t (in time units). One can then calculate from Eq. (12.8) the loss impedance for various cases.

For the case of a broad-band resonator with shunt impedance R_{bb}, quality factor Q_r and resonance frequency ω_r, the *broad-band loss impedance* Z_{bb} is given by

$$Z_{bb} = R_{bb}\left(\frac{\pi\,\omega_r}{Q_r\,\omega_0}\right) e^{-(\omega_r\sigma_t)^2}. \tag{12.31}$$

This expression is valid provided the bunch is short compared to the bunch spacing, and the resonator bandwidth is large compared to the bunch frequency $\omega_b \equiv M\omega_0$, namely $\omega_r/Q_r \gg \omega_b$. The bunches need not be equally spaced.

There is also power loss due to the HOMs of the RF cavities. In this case the resonators are narrowband, namely $\omega_r/Q_r \ll \omega_b$, and the formula is more complicated.[f] For a beam consisting of *M* equally-spaced bunches that are short compared to the bunch spacing, the *narrowband loss*

[f] In this case one must replace the integral in Eq. (12.8) by a summation over harmonics of the bunch frequency.

impedance Z_{nb} is given by[12]

$$Z_{nb} = 2MR_{S,r}\frac{\Delta^2 e^{-(\omega_r\sigma_t)^2}}{\sin^2\left(\pi\omega_r/\omega_b\right)+\Delta^2}. \tag{12.32}$$

where $R_{S,r}$ is the shunt impedance of the resonator, and $\Delta \equiv \pi\omega_r/2Q_r\omega_b$. Since, by definition, $\Delta \ll 1$, the above formula implies that the power loss is substantial only when ω_r/ω_b is very close to (within ~Δ of) an integer, namely when the resonance frequency of the HOM is very close to a harmonic of the bunch frequency. When this undesirable resonance condition is satisfied, the $\sin^2$-term in Eq. (12.32) vanishes, and the power loss is proportional to $M^2 I_b^2 = I_0^2$, which can be intolerably large. Fortunately, the very narrowness of the mode makes it easy to avoid this condition by a slight detuning of the HOM frequency.

The ohmic losses due to the resistivity of the vacuum chamber are, typically, smaller than those from the broad-band resonator described above. The *resistive wall loss impedance* Z_{rw} for a cylindrical pipe is obtained from Eq. (12.20) and is given by

$$Z_{rw} = \Gamma\left(\tfrac{3}{4}\right)Z_0\left(\frac{\delta(\omega_0)}{2b}\right)\left(\frac{R}{\sigma_z}\right)^{3/2} \tag{12.33}$$

where $\delta(\omega_0)$ is the skin depth at the revolution frequency, σ_z is the rms bunch length ($\sigma_z = c\sigma_t$), and $\Gamma(3/4) \approx 1.23$. The bunches need not be equally spaced.

12.4.3 Longitudinal Effects

It is possible for wake fields to drive coherent oscillations of the bunch shape and density. A general bunch distribution can be analyzed in terms of its radial and azimuthal moments in phase space. Radial modes are characterized by a radial variation of the distribution without an overall variation in shape, while azimuthal modes have the opposite characteristic. In Fig. 12.5 we sketch the first three azimuthal modes of oscillations in phase space along with the projection onto the time axis, which corresponds to the longitudinal charge density. Because each electron in the bunch is oscillating at the synchrotron frequency ω_s, one can see that the *m*-th mode has a characteristic angular oscillation frequency $m\omega_s$ (this index *m* should not be confused with the index *m* that labels impedances). The characteristic signals for radial modes can be found similar to the azimuthal modes.

As explained in Chapter 4, the synchrotron oscillations of individual electrons in a bunch are governed by the voltage in the RF cavity. However, the wake field leads, in effect, to a distortion of the RF voltage seen by the bunch. This is known as *potential well distortion,* and is sketched in Fig. 12.6.

The effective slope of the bunch voltage depends on the characteristic wavelength of the longitudinal wake function and on the length of the bunch. It is typical to assume a $Q = 1$ resonator form for the longitudinal impedance with resonant frequency equal to the cut-off frequency,

$\omega_r = \omega_c \equiv c/b$. This implies that,[2] for long bunches ($\sigma_z > b$), the effective voltage is usually such that the bunch is lengthened and the wake function is referred to as inductive. For short bunches, the bunch may be shortened, in which case the wake function is called capacitive. This is qualitatively illustrated in Fig. 12.7. The convolution of the $m = 0$ mode (which represents the distribution itself, rather than any of the moments) of the bunch with the reactive part of the broad-band impedance determines the bunch distortion. If the bunch is long, its frequency spectrum is significant only near zero frequency, where the impedance is inductive and the bunch consequently lengthens. For short bunches, the bunch spectrum extends beyond ω_c, where the impedance is capacitive. If the net effect is positive, there is bunch shortening.

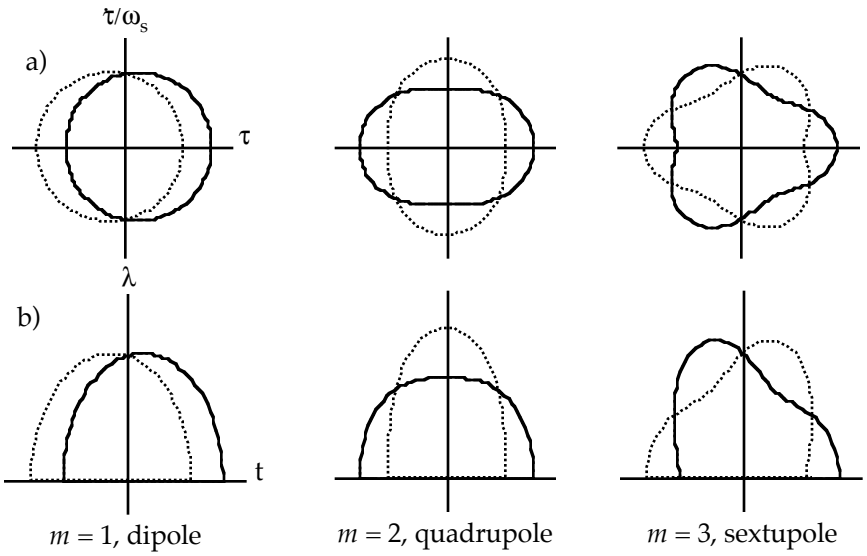

Fig. 12.5. Azimuthal bunch oscillation modes. The m-th mode has a characteristic frequency $m\omega_s$. The solid and dotted lines describe the distributions separated in time by $\pi/m\omega_s$. a) Phase space distribution. b) Line density vs. time.

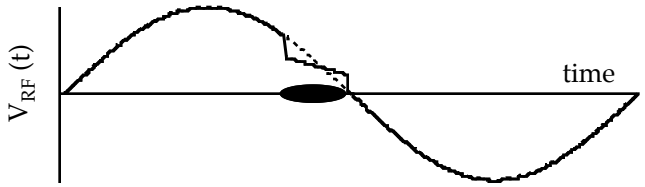

Fig. 12.6. The bunch wake field changes the effective slope of the RF voltage and can lead to bunch lengthening or shortening.

For azimuthal modes with $m \geq 1$, the wake fields also shift the coherent oscillation frequency away from its zero-current value $m\omega_s$. Like bunch lengthening, this frequency shift is determined by the convolution of the spectrum of the mode with the reactive part of the impedance. To first order approximation in the bunch current, this shift is not significant for the centroid of the

bunch ($m = 1$ mode) because the wake field moves along with the bunch. However, the effect can be observed by measuring the oscillation frequencies of higher azimuthal modes.

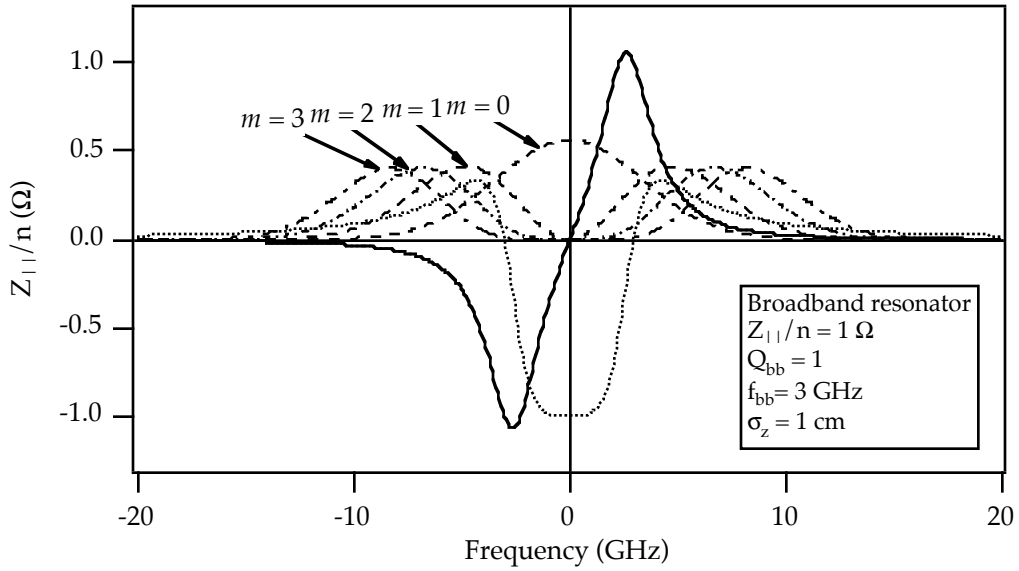

Fig. 12.7. The bunch spectrum for bunch oscillation modes m=0,...,3. The effective impedance for each mode is the sum over the broad-band impedance weighted by the bunch spectrum.

If the current is sufficiently high, the high-frequency components of the wake field can cause ripples in the longitudinal density that can amplify and grow exponentially, leading to an instability. For example, this happens to a coasting (unbunched) proton beam below transition energy (see Chapter 2) if the impedance is capacitive. This instability is called the *negative mass instability*. However, the energy spread in the beam leads to a spread in revolution frequency which, in turn, leads to Landau damping of the perturbation when the growth time is longer than the time necessary for the perturbation to dephase by 180 degrees. The stability limit on the total beam current is given by

$$I_0 < \frac{2\pi\eta(E/e)(\sigma_E/E)^2}{|Z_{\|}/n|_{bb}} \tag{12.34}$$

where e is the electronic charge, E is the beam energy, σ_E/E is the relative rms energy spread, and η is the phase-slip factor, related to the momentum compaction factor α by $\eta = \alpha - 1/\gamma^2$ (see Chapter 2). This relation is commonly referred to as the *Keil-Schnell criterion.*[13]

For bunched beams, this instability is called the *microwave instability*, or *turbulent bunch lengthening instability*. The Keil-Schnell criterion can be used in this case if the total beam current I_0 in Eq. (12.34) is replaced by the peak current, $\hat{I} = \sqrt{2\pi}\, I_b/\omega_0\sigma_t$. Thus the threshold for this instability, expressed in terms of the bunch current, is given by

$$I_{b,\mathrm{thr.}} = \sqrt{2\pi}\,\frac{\eta\,\omega_0\sigma_t(E/e)(\sigma_E/E)^2}{\left|Z_\parallel/n\right|_{bb}}. \tag{12.35}$$

If the current exceeds this threshold, both the bunch energy spread and the bunch length grow. This phenomenon is referred to as *turbulent bunch lengthening*. However, this growth stops when the peak current falls below the stability threshold, at which point a new equilibrium situation is reached, and the instability is said to saturate. The bunch length above threshold is given by

$$\sigma_z = \left(K\,I_b\left|Z_\parallel/n\right|_{bb}\right)^{1/3} \tag{12.36}$$

where K is given by

$$K = \frac{\eta\,R^3}{\sqrt{2\pi}(E/e)\nu_s^2} \tag{12.37}$$

and the energy spread is given by the usual formula, $\sigma_E/E = \nu_s\beta^2\sigma_z/\eta R$, where β is here the usual relativistic factor.

Eq. (12.35) assumes that $\left|Z_\parallel(\omega)/n\right|$ is independent of frequency, in accordance with the $Q=1$ broad-band resonator model. For the case of a more general broad-band impedance with a power-law frequency dependence of the form $Z_\parallel(\omega)\propto\omega^a$, it can be shown[2] that the bunch length has the dependence

$$\sigma_z \propto K^{1/(2+a)}. \tag{12.38}$$

An example of turbulent bunch lengthening from SPEAR[14] is shown in Fig. 12.8. The power law dependence of the bunch lengthening is clearly exhibited in the results, from which one can extract the value $a=-0.68$. This power-law dependence of the impedance is referred to as "SPEAR scaling," and it is valid only within a limited range of frequencies beyond cutoff. A similar measurement at the Photon Factory[15] yields $a=0.976$, showing that $\left|Z_\parallel(\omega)/n\right|$ is essentially independent of frequency in this case.

12.4.4 Transverse Effects

As in the longitudinal case, it is possible for wakefields to drive coherent transverse oscillations within the bunch. However, the situation for transverse oscillations is somewhat complicated by the constant exchange of the head and the tail of the bunch via longitudinal oscillations. Fortunately, this exchange provides a powerful mechanism for Landau damping of transverse oscillations.

Consider an extremely simplified model of a bunch consisting of two electrons, one at the head of the bunch, the other one at the tail. Without longitudinal oscillations, the transverse betatron oscillations of the head would generate a transverse wake field that would drive the tail of the bunch resonantly, as mentioned in Sec. 12.4.1. In the case of linacs, where the synchrotron motion is essentially frozen, this phenomenon leads to the *dipole beam breakup instability*. However, the longitudinal oscillations in circular

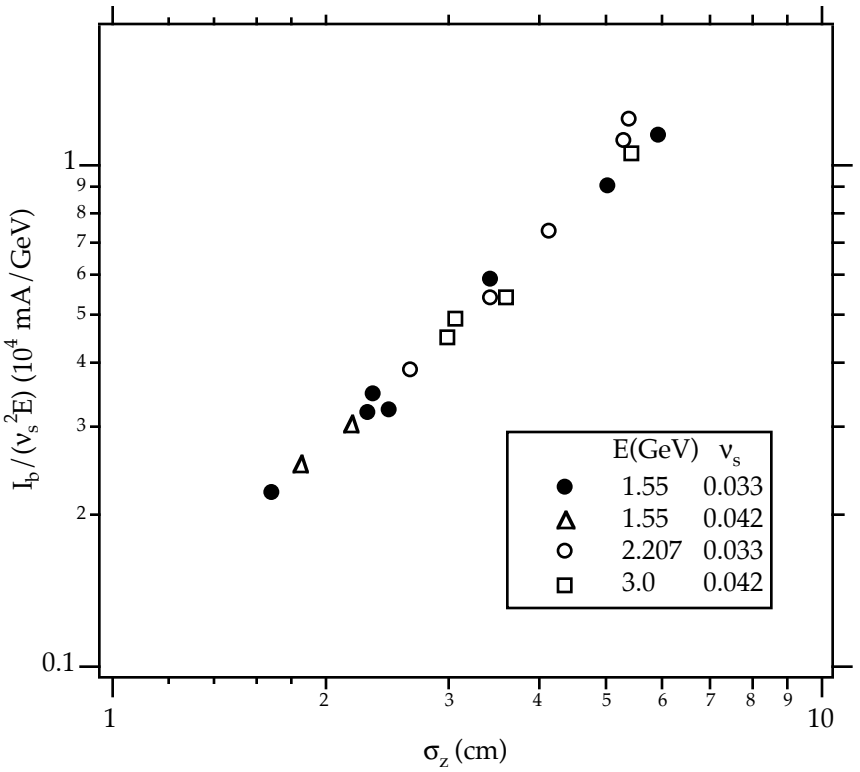

Fig. 12.8. Turbulent bunch lengthening measured at SPEAR.

accelerators cause the head and tail of the bunch to exchange places over a synchrotron period. This continuous exchange does not allow the growth of the oscillation amplitude of the tail to accumulate as quickly, thus extending the stability threshold. Obviously, if the transverse wake fields are so intense that the growth time of the oscillation amplitude of the tail is less than half a synchrotron period, the bunch becomes unstable and is quickly lost. This instability is variously referred to as *transverse mode-coupling instability*, or *fast head-tail instability*, or *transverse turbulent instability*. The threshold for the bunch current is given by

$$I_{b,\mathrm{thr.}} = \sqrt{2\pi}\,\frac{\eta(E/e)(\sigma_E/E)}{\left\langle \beta_\perp |Z_\perp|_{bb} \right\rangle} \tag{12.39}$$

where the denominator represents a ring average of the broad-band transverse impedance weighted by the lattice beta function. Typically, the threshold current for this instability is higher than its longitudinal counterpart, given by Eq. (12.35).

As in the case of longitudinal oscillations, it is customary to analyze the transverse oscillations of the bunch in terms of normal modes, referred to as head-tail modes. Each head-tail mode is specified by index $m = 0, \pm 1, \pm 2, \ldots$ (not to be confused with the longitudinal index or with the index of the impedance) which indicates the number of betatron wavelengths per synchrotron

period. For mode $m = 0$, all electrons have the same betatron phase (rigid dipole motion), whereas for $m = \pm 1$ the head and tail have opposite phases. The dipole signal for these two modes over several turns is shown in Fig. 12.9 (mode *m* has *m* nodes along the length of the bunch). Because of the constant exchange of the head and tail at the synchrotron frequency, each mode has a characteristic angular frequency $\omega_\beta + m\omega_s$. The frequency spectrum of the higher modes peaks at higher frequencies, similar to the longitudinal case described above.

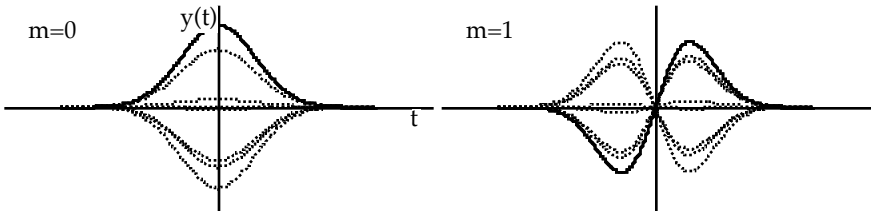

Fig. 12.9. Sketch of the *m*=0 and *m*=1 vertical modes of oscillation.

Under certain conditions, coherent bunch oscillations can be excited for currents below the instability threshold. An example of a coherent vertical head-tail oscillation observed at LEP with a streak camera is shown in Figure 12.10.

If the chromaticity is not zero (see Chapter 2), the energy spread of electrons leads to a modulation of the betatron tune at the synchrotron tune. This frequency modulation creates a relative phase shift between the head and the tail of the bunch. Because of this phase shift, the wake field produced by the head of the bunch no longer drives the tail on resonance. The corresponding impedance has a resistive part that can lead to damping or antidamping of the tail oscillation. This effect is referred to as *head-tail damping* and is used quite often to damp coherent transverse motion. Above transition energy, which is the typical situation for electron storage rings, the rigid transverse dipole mode ($m = 0$) is damped by positive chromaticity while the $m = \pm 1$ modes (head and tail out of phase) are antidamped. However, the growth rate must exceed the radiation damping rate for the beam to become unstable. This allows most electron storage rings to operate stably with a slightly positive chromaticity.

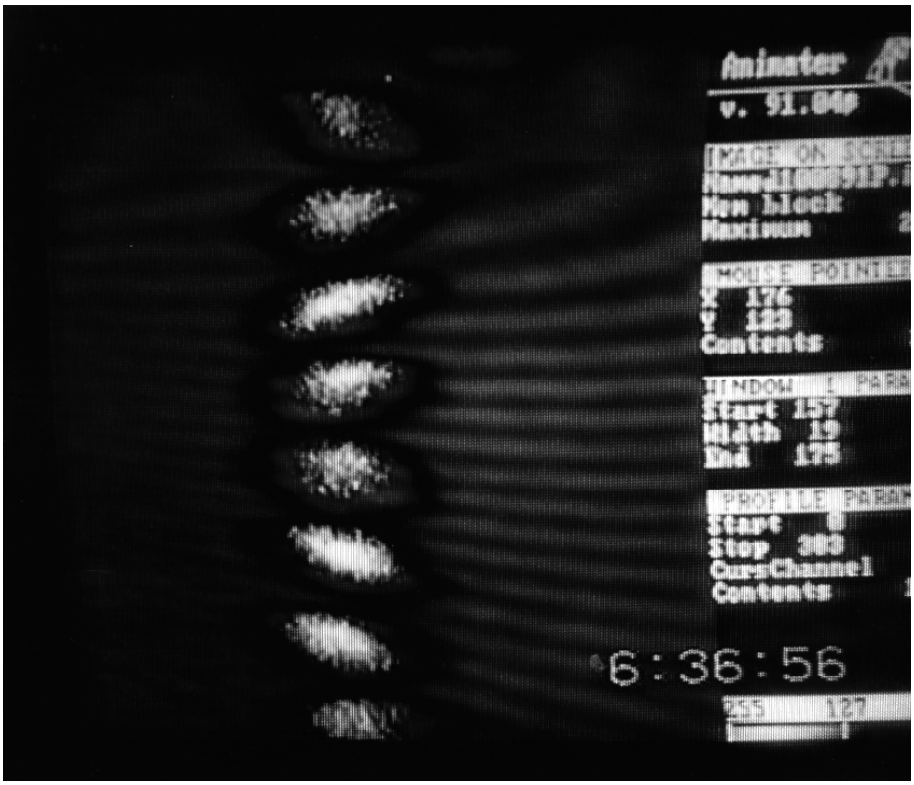

Fig. 12.10. Turn-by-turn pictures of a bunch executing vertical head-tail oscillations in the electron storage ring LEP. The bunch is observed from the side. The synchrotron tune is ~0.1. The horizontal scale is 1000 ps for the total image, not counting the table of numbers at the right. The vertical scale is uncalibrated, but the vertical rms beam size is ~0.2 mm at the observation point. Photo courtesy of E. Rossa.

12.5 Coupled-Bunch Instabilities[10,16]

12.5.1 Basics

Wake fields whose range is long enough to couple the motion of the different bunches in the beam can cause coupled-bunch instabilities. These wake fields are typically produced by narrow resonances in the RF cavities. Even though they remain localized in the cavities, they last for a long enough time that the motion of any given bunch is perturbed by all its predecessors. These long-lasting wake forces can generate a transverse or longitudinal coherent structure in the bunch-to-bunch oscillations. If these coherent oscillations grow indefinitely, they lead to rapid beam loss. If they remain bounded, they degrade the beam quality by inducing a larger effective beam size or oscillations in the arrival time.

Although it is possible for wakefields to couple the bunch shape oscillations from bunch to bunch, the scope of this section is limited to *dipole coupled-bunch oscillations* since these are the dominant concern for the design of a light source (or any other multibunch circular machine). These oscillations are characterized by the motion of the bunches about their nominal centers as if they were rigid "macroparticles." A sketch of a coherent transverse coupled-bunch oscillation is

shown in Fig. 12.11.

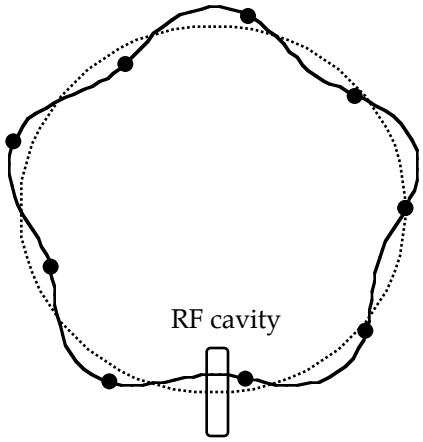

Fig. 12.11. Sketch of a coherent transverse coupled-bunch oscillation.

In analogy with the problem of coupled harmonic oscillators, it is best to analyze the motion of multibunch modes rather than that of individual bunches. The simplest case is that of a beam of M rigid, identical electron bunches spaced equally around the ring. For either transverse or longitudinal oscillations, each multibunch mode is characterized by a bunch-to-bunch phase difference of $\Delta\phi = 2\pi l/M$, where the mode number l can only take the values $l = 0,1,\ldots,M-1$. The net phase advance around the ring is constrained to be a multiple of 2π; when observed from a single point in the ring, each multibunch mode is associated with a characteristic set of frequencies given by

$$\omega_p = \left(pM \pm (l+\nu)\right)\omega_0 \tag{12.40}$$

where p is some integer and ν is either the synchrotron tune ν_s or the transverse tune ν_β, depending on whether the oscillations are longitudinal or transverse, respectively.

A snapshot view of a multibunch mode in the ring is illustrated in Fig. 12.12 for the case of M = 3 bunches. In this case, the longitudinal oscillations have relative phases $\Delta\phi = 2\pi/3$ or $\Delta\phi = 4\pi/3$ (multibunch modes $l = 1$ and $l = 2$, respectively). The corresponding waves are shown in Figs. 12.13a and 12.13b, and the resulting frequency spectrum in Fig. 12.14, where the modes appear as sidebands separated from the revolution harmonics by ν.

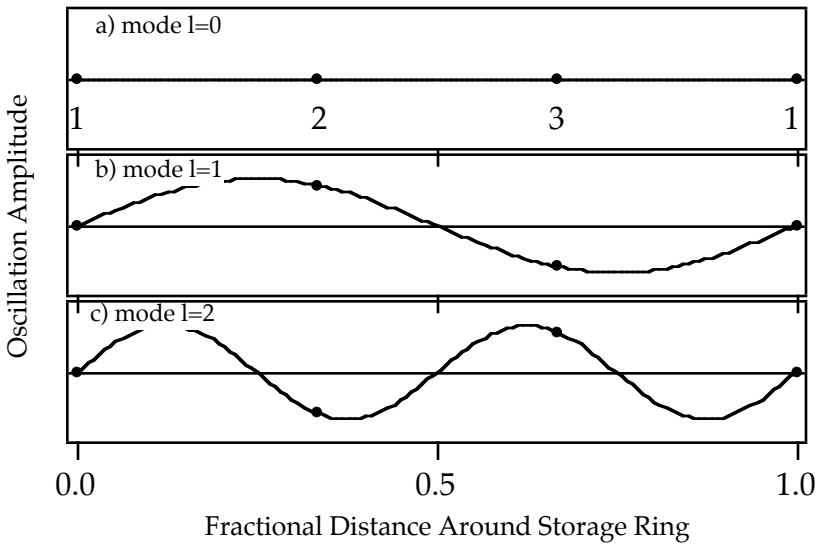

Fig. 12.12. Snapshot of a three-bunch beam executing multibunch oscillations.

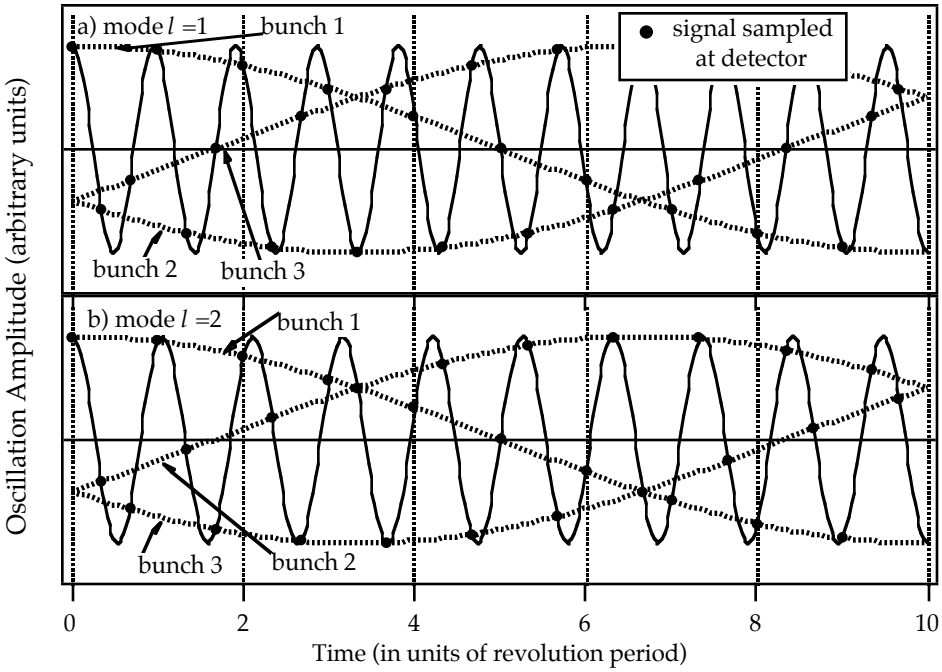

Fig. 12.13. An illustration of the characteristic signal at a fixed location in the ring for each multibunch mode. (a) Mode l=1. (b) Mode l=2. The dots represent the signal sampled at the detector. The thick dashed lines show the motion of individual bunches. The narrow, high frequency line shows the lowest frequency wave that fits the sampled measurement points.

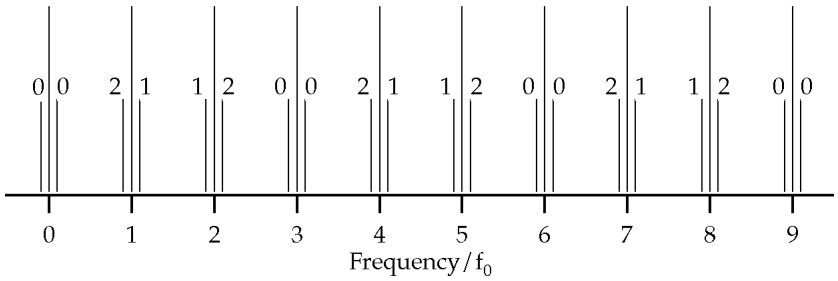

Fig. 12.14. Coupled-bunch mode spectrum for 3 bunches corresponding to Eq. (12.40). The sidebands are labeled with the corresponding coupled-bunch mode index. If the oscillations are longitudinal, the sidebands are split from the harmonics of the revolution frequency by $\pm\nu_s$; if transverse, by $\pm\nu_\beta$.

12.5.2 Longitudinal Coupled-Bunch Instability

It is useful to give a physical picture of a simple longitudinal coupled-bunch instability. Consider a single rigid bunch executing synchrotron oscillations; this bunch is in a storage ring containing an idle RF cavity with a single resonant mode whose frequency can be tuned over any desired range. In addition, the ring is assumed to have at least one other RF cavity that supplies power to the beam but has no other effects. For the sake of illustration, assume that the resonant frequency of the idle cavity is tuned to about twice the revolution frequency. As the beam passes through this element on some arbitrary turn, it induces a voltage that oscillates at the resonant frequency, as shown in Fig. 12.15a (a negative voltage implies deceleration of the bunch; the beam-induced voltage from subsequent passages of the bunch is not shown). During the half of the synchrotron oscillation when the energy of the bunch is smaller than the design energy, the revolution period[g] is shorter than nominal, and the bunch arrives at the idle cavity earlier than an on-energy bunch. The opposite is true during the half of the synchrotron oscillation when the energy of the bunch is greater than the design energy. In either case, the bunch sees the induced voltage from the previous turn as indicated.

In a first example, we assume that the frequency of the resonant mode of the idle cavity is slightly smaller than twice the revolution frequency. When the energy of the bunch is smaller than its design value, the bunch sees less decelerating voltage than when its energy is above the design value. Therefore, over the course of several turns, the energy oscillations of the bunch grows smaller and smaller. Thus the interaction with the resonator damps the oscillations and the motion is inherently stable. This effect is usually referred to as *Robinson damping*[17] when the resonator is the fundamental mode of the RF cavity.

In a second example, let the frequency of the resonant mode be tuned slightly above twice the revolution frequency. The relative arrival times are shifted relative to the previous case, as shown

[g] We assume that the ring is operated above transition energy since, in practice, this is the typical case.

in Fig. 12.15b. In this case, the below-energy bunch loses more energy than the above-energy bunch resulting in an unstable oscillation (if the ring happens to be operated below transition, the two cases are reversed).

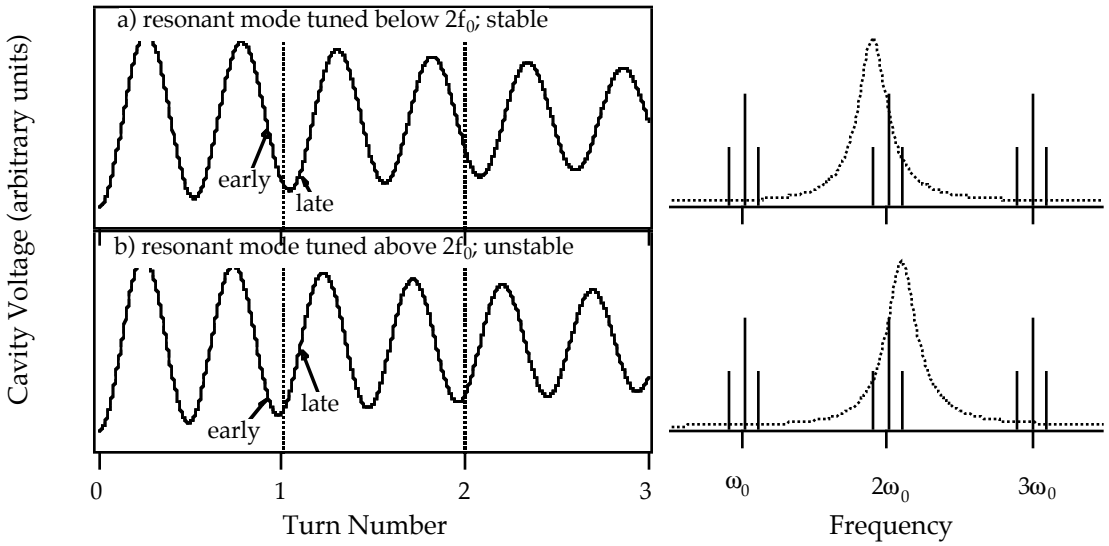

Fig. 12.15. A time-domain view of a resonator voltage driving a longitudinal coupled-bunch instability and the corresponding frequency domain view. The sidebands of the revolution harmonics represent the phase modulation of the beam current resulting from the synchrotron oscillations, and the dashed line is the resistive part of a resonator impedance.

Although this simplified description gives a view of the interaction of the bunch with its own voltage over the course of two revolutions, it is inadequate for the description of the multi-turn cumulative effect. For instance, the net beam-induced voltage in the example above might sum to zero over the course of many turns, or the beam-induced voltage from other bunches in the beam might cancel the voltage from the first bunch. The above treatment also implies a point-like charge. In reality, electron bunches have a distribution in their energy, position, and synchrotron frequency, and beam wake fields can affect the electrons within the bunch.

The obvious difficulties of understanding the summation of beam-induced voltages and the resulting effects on a bunched beam over many turns are greatly simplified by analyzing the problem in the frequency domain. Consider the frequency spectrum of a single bunch and the resistive part of a resonator impedance as shown in Fig. 12.15. The revolution frequency of the bunch increases (decreases) when its energy is greater than (smaller than) the design energy, corresponding, respectively, to the lower and upper sidebands. The energy absorbed by the resonant mode is proportional to the resistive part of the impedance at the frequency of the sideband. When the idle cavity is tuned to the RF frequency, it absorbs the same energy from the upper and lower sidebands. In other words, it absorbs the same energy from the bunch when it is below energy as it does when the bunch is above energy. When the cavity is tuned below a multiple of the revolution

frequency, as shown in Fig. 12.15a, it absorbs more energy from the bunch when it is above the design energy than when it is below, and is thus stable. But if the resonant mode is tuned above a multiple of the revolution frequency, as shown in Fig. 12.15b, the situation is reversed and the energy oscillations of the bunch are antidamped.

In general, as mentioned earlier, the interaction of the beam with the wake fields leads to both an amplitude growth and a frequency shift of the longitudinal beam oscillations. For coupled-bunch mode l the *complex coherent frequency shift* is given by

$$\Delta\Omega_{\|}^{l} = i\frac{\eta h\omega_0 I_0}{4\pi\nu_s(E/e)}\left[Z_{\|}\right]_{\text{eff.}}^{l} \tag{12.41}$$

where the effective impedance is the sum of the impedance weighted by the beam spectrum, and is given by

$$\left[Z_{\|}\right]_{\text{eff.}}^{l} = \sum_{p=-\infty}^{\infty}\frac{\omega_p}{\omega_{RF}}Z_{\|}(\omega_p)e^{-(\omega_p\sigma_\tau)^2} \tag{12.42}$$

and where $\omega_p \equiv (pM + l + \nu_s)\omega_0$.

The real part of $\Delta\Omega$ yields the shift in the oscillation frequency of the mode, and is driven by the reactive part of the impedance. The imaginary part is the growth rate of the oscillation, and is driven by the resistive part of the impedance. Note that higher frequency resonators have a stronger effect on longitudinal motion because the phase modulation of the beam is larger at higher frequencies. The motion becomes unstable when the growth rate is positive and exceeds the sum of the radiation and Landau damping rates.

For example, in the case of a single high-Q resonator tuned near the frequency $pM\omega_0$, a bunch whose length is short compared to the wavelength of the resonator has a growth rate given by

$$\frac{1}{\tau_{\|,l}} = \frac{\eta h\omega_0 I_0 R_{\text{eff.}\|,l}}{4\pi\nu_s(E/e)} \tag{12.43}$$

where

$$\begin{aligned} R_{\text{eff.}\|,l} = \text{Re}\left[Z_{\|}\right]_{\text{eff.}}^{l} \approx (pM + l + \nu_s)\,\text{Re}\,Z_{\|}\big((pM + l + \nu_s)\omega_0\big)/h - \\ (pM - l - \nu_s)\,\text{Re}\,Z_{\|}\big((pM - l - \nu_s)\omega_0\big)/h. \end{aligned} \tag{12.44}$$

In other words, the growth rate is proportional to the difference in impedance between the upper and lower sidebands of the coupled-bunch mode in question. This agrees with the qualitative argument given above.

In actual storage rings which observe longitudinal instabilities, the oscillations typically grow to an amplitude where some other damping mechanism such as Landau damping limits further growth. Finite-amplitude longitudinal oscillations[18] can affect the average beam size at a point in the lattice with dispersion and thus the average brightness of the photon beam. Furthermore, because of the high magnetic quality of modern insertion devices, the spectral width of

higher harmonics of the synchrotron light is sensitive to energy oscillations, even if there is no effective increase in the transverse beam size, as exemplified in initial measurements at the ALS shown in Fig 12.16. The top graph shows a measurement of the electron beam spectrum from a BPM sum signal near several revolution harmonics with all RF buckets filled. The central peaks are revolution harmonics with phase modulation sidebands indicating large amplitude coupled-bunch longitudinal oscillations. The bottom graph shows significant spectral broadening of the synchrotron radiation at the undulator third harmonic in multibunch mode vs. single bunch mode.

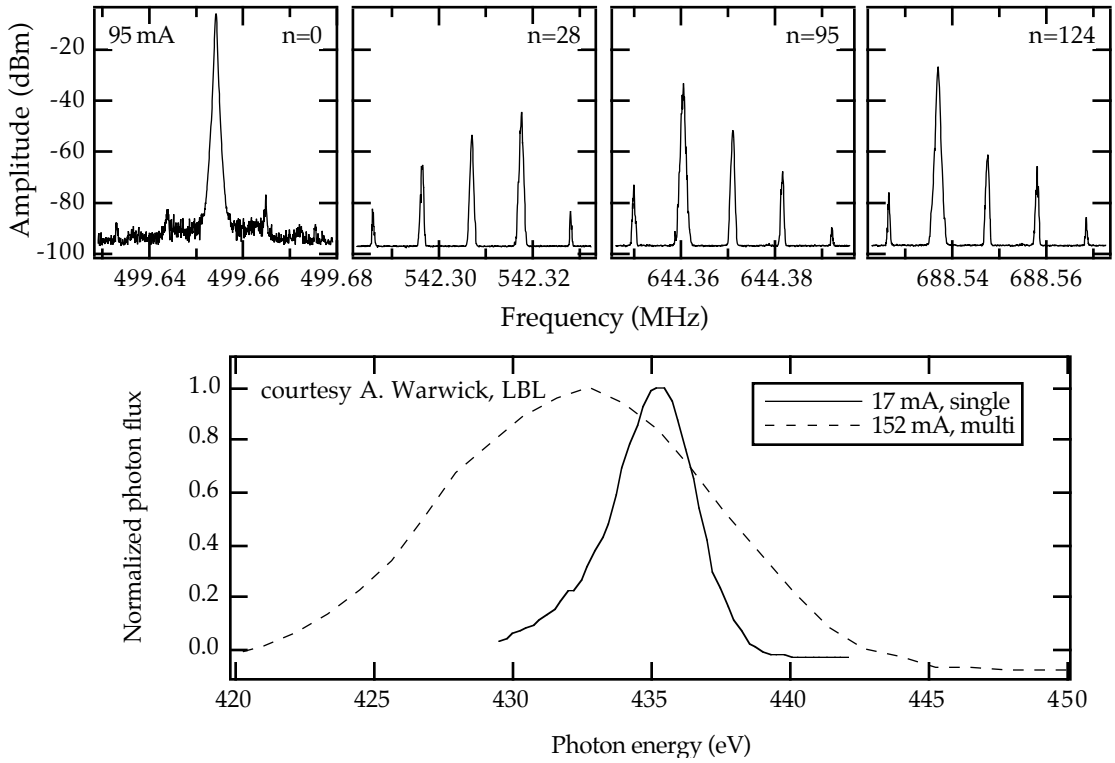

Fig. 12.16. The ALS electron beam spectrum near several revolution harmonics with all RF buckets filled indicates large amplitude longtitudinal coupled-bunch oscillations. The central peak in each graph is the signal at the nth revolution harmonic above the RF frequency and the phase modulation sidebands are oscillations of various normal modes of the beam. The bottom graph shows initial measurements of the undulator 3rd harmonic taken under similar conditions during the commissioning of an ALS undulator. A marked increase in the spectral width of higher harmonics of the synchrotron light results from the coupled-bunch energy oscillations.

12.5.3 Transverse Coupled-Bunch Instability

Transverse instabilities are driven by narrow-band dipole HOMs of the RF cavity and also by the resistive wall impedance. For low frequencies, the skin depth is relatively large and hence the wake field can last for a sufficiently long time to couple the motion of different bunches. Since the transverse impedance scales with the chamber radius as b^{-3} (viz. Eqs. (12.6) and (12.20)), it is of particular concern for future light sources which require small chamber sizes to accommodate strong insertion devices.

The physical mechanism for the transverse coupled-bunch instabilities is similar to that for longitudinal instabilities. The transverse complex frequency shift for coupled-bunch mode *l* and dipole head-tail mode (rigid bunch shape) is given by

$$\Delta\Omega_{\perp}^{l} = -i\frac{\omega_0 I_0 \beta_{\perp}}{4\pi(E/e)}\left[Z_{\perp}\right]_{\text{eff.}}^{l} \tag{12.45}$$

where

$$\left[Z_{\perp}\right]_{\text{eff.}}^{l} = \sum_{p=-\infty}^{\infty} Z_{\perp}(\omega_p)e^{-(\omega_{\xi}\sigma_t)^2}\,. \tag{12.46}$$

Here $\omega_p \equiv (pM + l + \nu_{\perp})\omega_0$, $\omega_{\xi} \equiv (pM + l + \nu_{\perp} - \xi/\eta)\omega_0$, ξ is the chromaticity, $\beta_{\perp}$ is the beta function (*x* or *y*) at the location of the impedance, and $\nu_{\perp}$ is the transverse tune. In the case of a single high-*Q* resonator tuned near the frequency $pM\omega_0$, with zero chromaticity and a bunch length short compared to the resonant wavelength of the resonator, the growth rate is given by

$$\frac{1}{\tau_{\perp,l}} = \frac{\omega_0 I_0 R_{\text{eff.}\perp,l}}{4\pi(E/e)} \tag{12.47}$$

where

$$R_{\text{eff.}\perp,l} = -\beta_{\perp}\,\text{Re}\left[Z_{\perp}\left((pM + l + \nu_{\perp})\omega_0\right) - Z_{\perp}\left((pM - l - \nu_{\perp})\omega_0\right)\right]. \tag{12.48}$$

12.5.4 Coupled-Bunch Instability Cures[19]

The most obvious remedy for coupled-bunch instabilities is to eliminate or reduce the strength of the HOMs in the design of the RF cavity. However, this reduction usually comes at the expense of the strength of the fundamental mode, thus requiring more total RF power to supply the requisite voltage to the beam. Tuned antennae can be used to couple energy out of the cavity if there is only a single troublesome HOM. Another method is to adjust the frequencies of the HOMs such that they lie in between harmful beam resonant frequencies. However, because the minimum spacing between these frequencies is ω_0, this method is possible only for HOMs with bandwidths much smaller than ω_0. Furthermore, the HOM frequencies shift with changes in the cavity temperature and the position of the tuning rod, thus making them difficult to control. For a storage ring with multiple RF cavities, it is possible to arrange the HOM frequencies of each cavity so that they do not coincide with each other, thus reducing the scale of the problem. Another method is to increase the effect of Landau damping by increasing the effective synchrotron or betatron tune spread. This can be accomplished in the longitudinal plane by either running the RF cavity at lower voltage and thus at longer bunch length, or by adding a higher harmonic RF cavity. The tune spread in the transverse plane can be increased by adding octupole magnets to the storage ring lattice. A variation on this scheme is to create a bunch-to-bunch synchrotron or betatron tune spread by modulating the RF voltage or by using an RF quadrupole.[20] A bunch-to-bunch synchrotron tune spread can also be generated by transient beam loading effects induced by gaps in the beam.

Finally, the most powerful method is to add an active feedback system which senses the oscillation of each bunch and provides a corrective kick on the following turn. The cure for coupled-bunch instabilities in a storage ring is usually a combination of all of the above.

12.6 Trapped Ions and Beam Lifetime Issues

12.6.1 Trapped Ions[21]

Positive ions are created when the beam ionizes the gas molecules remaining in the vacuum chamber. Since the beam is negatively charged, the ions remain trapped in the electric potential well of the beam. Possible consequences from this are: reduced beam lifetime due to multiple scattering, tune spread, emittance increase, and electron-ion coherent oscillations. Ion trapping is a poorly understood phenomenon, and has been observed in all synchrotron light sources operating in multibunch mode and in many other electron storage rings. An obvious way to avoid ion trapping altogether is to use positrons rather than electrons in the beam. This solution, however, requires a positron source, which is typically quite expensive. More typical solutions are described below.

Near the beam center, a trapped ion with net charge Ze and atomic number A oscillates vertically in the potential well of an electron beam of total current I_0 with an average angular frequency given by

$$\omega_y^2 = \frac{2Ze}{m_p cA} \cdot \frac{I_0}{\sigma_y\left(\sigma_x + \sigma_y\right)} \tag{12.49}$$

with a corresponding horizontal frequency obtained from the above by the exchange $\sigma_y \leftrightarrow \sigma_x$. In this expression m_p is the proton mass and σ_x and σ_y are the horizontal and vertical rms sizes of the bunch, respectively, at the ring location where the ion is trapped. By applying linear transport theory to the motion of the ions, one can derive a condition for the ions to be stably trapped. For a beam with a uniform bunch population, the condition is

$$\left(\omega_y \Delta t\right)^2 < 4 \tag{12.50}$$

where Δt is the bunch separation in time (it is only necessary to consider the vertical oscillations because, typically, $\sigma_y \ll \sigma_x$ and therefore $\omega_y \gg \omega_x$). This condition implies that all ions with a mass-to-charge ratio larger than a critical value,

$$\frac{A}{Z} > \left(\frac{A}{Z}\right)_c \equiv \frac{\pi R N r_p}{M\sigma_y\left(\sigma_x + \sigma_y\right)} \tag{12.51}$$

will be trapped. Here $r_p \equiv e^2/m_p c^2 \approx 1.535 \times 10^{-18}$ m is the classical proton radius, N is the number of electrons per bunch, and M is the number of bunches in the beam.

If no steps are taken to clear the ions, they progressively accumulate and neutralize the electron beam. As a result, the value of N in Eq. (12.51) effectively decreases and $(A/Z)_c$ becomes smaller, so that ions with lower and lower A/Z ratios can become trapped in turn. This

phenomenon is known as the *ion ladder*.

Since $\sigma_y \ll \sigma_x$ the potential well is much deeper in the vertical direction than in the horizontal, and it is deepest where σ_y is smallest, namely near the defocusing quadrupole magnets in the ring. As a result, ions tend to get preferentially trapped at these locations. One way to eliminate these ions is by means of clearing electrodes, typically placed near the defocusing quadrupoles. For low beam currents, a DC voltage of a few kV is usually sufficient to pull the ions away from the potential well. For large beam currents the required voltage might be too large and thus this technique might be impractical or detrimental to the electron beam. In this case, ion clearing is more effective if the electrode voltage has an AC component whose frequency is equal to the ion frequency given by Eq. (12.49), in addition to a DC component. In addition, for beams with many bunches, another method to clear ions is to leave a gap in the bunch train typically equivalent to ~10% of the beam. This *ion-clearing gap* leads to instabilities in the ion motion that are analogous to the betatron motion stopbands arising from resonances in a particle beam. In practice, a combination of all these methods is required.

12.6.2 Intrabeam and Touschek Scattering[22,23]

As time progresses, the particles within a bunch in a stored beam scatter off each other via the Coulomb force, exciting transverse and longitudinal oscillations. As a result of multiple small-angle scattering, particles diffuse in phase space causing a redistribution of all three emittances. This emittance redistribution is usually referred to as the *intrabeam scattering effect*. In addition, on rare occasions, the scattering involves wide angles and, as a result, a particle can fall outside the dynamic aperture or the energy acceptance of the machine, and gets lost. This beam lifetime limitation due to occasional large-angle Coulomb scattering is usually referred to as the *Touschek effect*. Obviously there is no conceptual difference between the two effects. However, since they lead to different manifestations in the beam dynamics, they are traditionally analyzed separately. In the case of the intrabeam scattering effect, the quantities of interest are the damping (or growth) rates for the three emittances; in the case of the Touschek effect, the quantity of interest is the beam lifetime.

Clearly, both effects have a strong dependence on beam energy, becoming more pronounced at lower energies. This can be qualitatively understood by noting that, in the Lab frame of reference, the electric and magnetic forces on any given particle almost cancel each other out at high energies, leaving a net Lorentz force proportional to γ^{-2} (γ is here the usual relativistic factor). As a result, typically, neither the intrabeam effect or the Touschek effect leads to significant problems in the operation of storage rings at energies $\gtrsim$ 1 GeV. However, both effects scale unfavorably with the beam density $N/\sigma_x\sigma_y\sigma_z$, where the σ's are the rms beam sizes. Therefore these effects can become important for modern light sources, which emphasize intense, small bunches.

In all light sources, and indeed in all storage rings built so far, the particle motion is, on average, nonrelativistic in the beam rest frame. In this frame, typically the horizontal and vertical

energy spreads are larger than the longitudinal. Therefore small-angle Coulomb scattering predominantly transfers energy from the transverse motion to the longitudinal, leading one to expect damping of the transverse emittances at the expense of growth of the longitudinal. However, a change in the particle energy excites, in turn, horizontal motion due to the dispersion in the ring. Typically, this effect more than compensates the damping of the horizontal emittance, and the net result is a damping of the vertical emittance and growth of both horizontal and longitudinal emittances. During this process, the quantity

$$-\eta\left(\sigma_E/E\right)^2+\varepsilon_x/\bar{\beta}_x+\varepsilon_y/\bar{\beta}_y \tag{12.52}$$

remains invariant, where the ε's are the emittances and the $\bar{\beta}$'s are the ring-averaged beta functions.

The Touschek lifetime is given by

$$\frac{1}{\tau}=\frac{r_e^2 cN}{8\pi\gamma^5\sigma_{x'}^3\sigma_x\sigma_y\sigma_z}\cdot\frac{F(\delta)}{\delta} \tag{12.53}$$

where $\sigma_{x'}$ is the rms of the beam divergence, and δ is defined by

$$\delta=\left(\frac{\Delta p/p}{\gamma\sigma_{x'}}\right)^2 \tag{12.54}$$

where $\Delta p/p$ is the momentum acceptance of the machine, which is determined, in turn, by the smallest of the RF bucket height or the energy aperture of the ring. The function $F(\delta)$ depends weakly on δ for small δ. For the range $\delta\lesssim 10^{-2}$, which is typical, it is given by

$$F(\delta)\approx-\ln(\gamma_e\delta)-3/2 \tag{12.55}$$

where $\gamma_e\approx 1.78$ is Euler's constant.

12.7 Acknowledgments

We are grateful to A. Chao, J. Corlett, M. Cornacchia, A. Hofmann, G. Lambertson, H. Winick and B. Zotter for valuable discussions. We are indebted to E. Rossa for providing the photo on Fig. 12.10.

12.8 References

1. S. Chattopadhyay, "Stability of High-Brilliance Synchrotron Radiation Sources," NIMPR **A291**, 455 (1990).
2. A. W. Chao, *Physics of Collective Beam Instabilities in High Energy Accelerators*, J. Wiley & Sons, 1993.
3. *Synchro-Betatron Resonances*, Proc. 6th Advanced ICFS Beam Dynamics Workshop, Madeira, Portugal, October 24–30, 1993, to be published.
4. *Impedance Beyond Cutoff*, Part. Accel. **25** nos. 2–4 (1990), S. Chattopadhyay, guest editor.
5. F. Caspers, "Bench Methods for Beam-Coupling Impedance Measurement," Proc. US-CERN School on Particle Accelerators, Hilton Head Island, S. Carolina, USA, Nov. 7–14, 1990, M. Month, E. Dienes and S. Turner (Eds.), Springer Verlag LNP **400**, p. 80.
6. T. Weiland and R. Wanzenberg, "Wake Fields and Impedances," *ibid.*, p. 39.
7. P. Schoessow, E. Chojnacki, W. Gai, C. Ho, R. Konecny, J. Power, M. Rosing and J. Simpson, "The Argonne Wakefield Accelerator–Overview and Status," Proc. IEEE Part. Accel. Conf., Washington, DC, May 17–20, 1993, p. 2596.
8. L. Landau, "On the Vibration of the Electric Plasma," J. Phys. (USSR) 10, **25** (1946).
9. H. G. Hereward, "The Elementary Theory of Landau Damping," CERN 65-20 (1965).
10. J. Gareyte, "Observation and Correction of Instabilities in Circular Accelerators," Ref. 5, p. 134.
11. M. S. Zisman, S. Chattopadhyay and J. J. Bisognano, "ZAP User's Manual," LBL-21270/UC-28, December 1986.
12. M. Furman, H. Lee and B. Zotter, "Energy Loss of Bunched Beam in SSC RF Cavities," Proc. 1987 Particle Accelerator Conference, Washington, DC, March 16–19, 1987, p. 1049.
13. E. Keil and W. Schnell, "Concerning Longitudinal Stability in the ISR," ISR-TH-RF/69-48 (1969); V. K. Neil and A. M. Sessler, "Longitudinal Resistive Instabilities of Intense Coasting Beams in Particle Accelerators," Rev. Sci. Inst. **36**, 429 (1965).
14. A. W. Chao and J. Gareyte, "Scaling Law for Bunch Lengthening in SPEAR II," Ref. 4, p. 229.
15. N. Nakamura, S. Sakanaka, K. Haga, M. Izawa and T. Katsura, "Collective Effects in Single Bunch Mode at the Photon Factory Storage Ring," Proc. IEEE Part. Accel. Conf., S. Francisco, CA, May 6–9, 1991, p. 440.
16. F. Sacherer, "A Longitudinal Stability Criterion for Bunched Beams," IEEE Trans. Nucl. Sci. **NS-20-3**, 825 (1973); A. Hofmann, "Coherent Beam Instabilities," Ref. 5, p. 110.
17. K. Robinson, "Stability of Beam in Radio-Frequency Systems," CEAL-1010 (1964).
18. J. Byrd, "Measurement of Collective Effects at the ALS," LBL-34954a/CBP Note 054, submitted to the 1994 European Part. Accel. Conf., London, June 27–July 1st, 1994.

19. F. Pedersen, “Multibunch Instabilities,” Proc. Joint US-CERN School on Particle Accelerators, Benalmádena, Spain, Oct. 29–Nov. 4, 1992, M. Dienes, M. Month, B. Strasser and S. Turner (Eds.), Springer Verlag LNP **425**, p. 269.
20. S. Sakanaka, T. Mitsuhashi, A. Ueda and M. Izawa, “Construction of a High-Frequency Quadrupole Magnet Used to Cure Transverse Coupled-Bunch Instabilities,” NIMPR **A325**, 1 (1993).
21. A. Poncet, “Ion Trapping and Clearing,” Ref. 19, p. 202; M. Cornacchia, “Requirements and Limitations on Beam Quality in Synchrotron Radiation Sources,” Proc. CAS on Synchrotron Radiation and FELs, Chester College, UK, Apr. 6-13, 1989, S. Turner (Ed.), CERN 90-03, p. 53.
22. A. Piwinski, “Intra-Beam Scattering,” Proc. Joint US-CERN School on Particle Accelerators, S. Padre Island, Texas, USA, Oct. 23-29, 1986, M. Month and S. Turner (Eds.), Springer Verlag LNP **296**, p. 297.
23. H. Brück, *Circular Particle Accelerators*, LASL Translation LA-TR-72-10 Rev., 1972.